

A Survey on Class-Agnostic Counting: Advancements from Reference-Based to Open-World Text-Guided Approaches

Luca Ciampi¹, Ali Azmoudeh², Elif Ecem Akbaba², Erdi Sarıtaş², Ziya Ata Yazıcı²,
Hazım Kemal Ekenel^{2,3}, Giuseppe Amato¹, Fabrizio Falchi¹

¹CNR-ISTI, Pisa, Italy ²Istanbul Technical University, Türkiye ³Division of Engineering, NYU Abu Dhabi, UAE

Abstract—Visual object counting has recently shifted towards class-agnostic counting (CAC), which addresses the challenge of counting objects across arbitrary categories—a crucial capability for flexible and generalizable counting systems. Unlike humans, who effortlessly identify and count objects from diverse categories without prior knowledge, most existing counting methods are restricted to enumerating instances of known classes, requiring extensive labeled datasets for training and struggling in open-vocabulary settings. In contrast, CAC aims to count objects belonging to classes never seen during training, operating in a few-shot setting. In this paper, we present the first comprehensive review of CAC methodologies. We propose a taxonomy to categorize CAC approaches into three paradigms based on how target object classes can be specified: reference-based, reference-less, and open-world text-guided. Reference-based approaches achieve state-of-the-art performance by relying on exemplar-guided mechanisms. Reference-less methods eliminate exemplar dependency by leveraging inherent image patterns. Finally, open-world text-guided methods use vision-language models, enabling object class descriptions via textual prompts, offering a flexible and promising solution. Based on this taxonomy, we provide an overview of 30 CAC architectures and report their performance on gold-standard benchmarks, discussing key strengths and limitations. Specifically, we present results on the FSC-147 dataset, setting a leaderboard using gold-standard metrics, and on the CARPK dataset to assess generalization capabilities. Finally, we offer a critical discussion of persistent challenges, such as annotation dependency and generalization, alongside future directions. We believe this survey offers a valuable resource for researchers, capturing the evolution of CAC and providing insights to guide future developments in the field.

Index Terms—Object Counting, Class-agnostic Counting, Few-shot Counting, Prompt-based Counting, Deep Learning, Survey

I. INTRODUCTION

The goal of object counting is to automatically estimate the number of object instances in still images or video frames [1]. This challenging task has emerged as a prominent research focus within the realm of computer vision, owing to its vast array of practical applications and interdisciplinary significance.

This work was partially funded by: Spoke 8, Tuscany Health Ecosystem (THE) Project (CUP B83C22003930001), funded by the National Recovery and Resilience Plan (NRRP), within the NextGeneration Europe (NGEU) Program; Horizon Europe Research & Innovation Programme under Grant agreement N. 101092612 (Social and hUman ceNtered XR - SUN project); PNRR - M4C2 - Investimento 1.3, Partenariato Esteso PE00000013 - "FAIR - Future Artificial Intelligence Research" - Spoke 1 "Human-centered AI", funded by European Union NextGenerationEU.

For instance, in crowd analysis [2], [3], [4], [5], [6], [7], [8], [9], [10], [11], it supports event monitoring with implications across social [12], psychological [13], political [14], and security domains [15]. In agriculture, it enables livestock and pest monitoring [16], [17], [18], and plant emergence assessment [19], [20], [21]. Other applications include traffic analysis [22], [23], [24], [25], [26], inventory control [27], and biomedical imaging [28], [29], [30], [31]. However, unlike humans—who can naturally identify what is worth counting and recognize repetitions even among unfamiliar objects—most AI-based methods are constrained to predefined categories. These approaches typically rely on prior knowledge of the object class and require dedicated models trained on large annotated datasets [32] (see also the left part of Fig. 1). Even recent general-purpose agents and MLLMs, such as LLaVA [33], MiniGPT4 [34], and mPLUG-owl [35], struggle with counting objects from open-vocabulary categories [36].

Very recently, research about object counting has shifted towards a new trend that aims to consider arbitrary object categories and attempts to alleviate the problem of the annotation burden (see right part of Fig. 1). The first attempt of creating a model able to count any class, i.e., to perform Class-Agnostic Counting (CAC), was proposed by Lu and Zisserman through the Generic Matching Network (GMN) [37], which formulates counting as a matching task by exploiting image self-similarity—since objects to be counted often repeat within the same image. GMN is pre-trained on tracking data and includes an adaptation module for domain transfer. However, this module requires dozens to hundreds of examples and performs poorly on novel classes without adaptation. The first work to significantly depart from standard class-specific counting was introduced by Ranjan et al. [32], who introduced a few-shot regression approach to counting. In this setting, the inputs are an image and a set of exemplars—bounding boxes around objects of interest from the same image—used as object prototypes. At inference time, similar to the few-shot classification paradigm [38], [39], the objects to be counted belong to unseen categories, making few-shot counting fundamentally different from traditional counting, where training and test classes match. Notably, this paradigm does not learn from limited data via domain adaptation [40], [41] or uncertainty modeling [42], but instead uses supervised data to train a class-agnostic model applicable to novel categories—

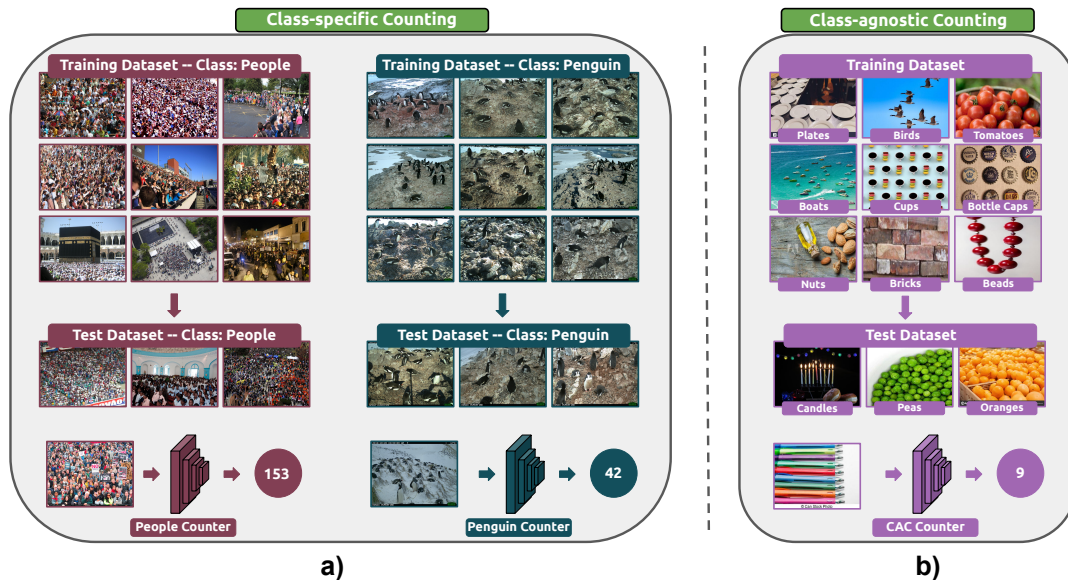


Fig. 1. **Comparison between class-specific and class-agnostic counting.** On the left, we show examples of class-specific counting, where each object category (e.g., cars, people, animals) requires a dedicated model trained on large, annotated datasets. These models are tailored to recognize and count only the specific class they were trained on. On the right, we present the class-agnostic counting approach, which aims to estimate the number of objects regardless of their semantic category. In this setting, the counting model is trained on a set of object classes and evaluated on entirely different, unseen classes, demonstrating its ability to generalize across categories. This paradigm significantly reduces the need for exhaustive per-class annotations and enables broader applicability in real-world scenarios.

making it data-efficient for unseen classes.

For the first time, this survey explores and analyzes the leading works existing in the literature tackling class-agnostic counting. Despite being a recent task, it has already attracted attention from top-tier venues, yielding progressively better results. Furthermore, its formulation has slightly changed and evolved compared to its original version, gradually reducing human intervention in the overall process, i.e., the need for annotated exemplars, either at training or inference time. In this context, our contributions are fourfold: (i) we propose a taxonomy to categorize CAC methods, bringing clarity to the literature; (ii) we provide an overview of the architectures of 30 CAC approaches; (iii) we present and compare the performance of the examined techniques on gold-standard benchmarks; (iv) we critically discuss the results from multiple perspectives.

Specifically, the proposed taxonomy organizes the surveyed CAC methods into three categories, also illustrated in Fig. 2. The first category follows the previously mentioned *reference-based* or *few-shot* paradigm [32], where annotated bounding box exemplars are required during both training and inference. Subsequently, CAC evolved into a formulation that shapes our second category, where manually specifying object categories is no longer necessary; the algorithm automatically identifies the dominant class(es) to be counted. This approach is known in the literature as *reference-less* or *exemplar-free*. Finally, the most recent paradigm, referred to as *open-world text-guided*, *prompt-based*, or *zero-shot*, allows the system to take natural language descriptions of object classes as input, going hand in hand with the latest vision-language foundation models, and constitutes our third category. These three paradigms reflect the evolution of CAC methodologies toward reduced

human supervision and increased flexibility. Reference-based methods, while effective, are not well-suited for autonomous systems, as they require users to manually provide exemplar inputs for each new category at inference time. Reference-less approaches address this limitation by removing the need for exemplars altogether, inferring the dominant object class directly from image patterns. However, they still lack semantic control and cannot incorporate user intent, making them suitable only when the target class aligns with the most visually repetitive category in the scene. Text-guided methods extend this trajectory by introducing a more natural and flexible way to specify the target category—closer to how humans describe objects—while leveraging the semantic capabilities of textual prompts. Rather than forming isolated categories, each paradigm represents a conceptual step forward, progressively addressing the limitations of the previous one and contributing to a more flexible and interaction-aware framework for CAC.

Based on this taxonomy, we present an overview of the architectures of the examined methods and show their performance on established benchmarks from the literature. In particular, we consider the FSC-147 dataset [32], introduced together with the few-shot CAC formulation and now regarded as the gold-standard benchmark for this task. FSC-147 includes over 6,000 images across 147 object categories. We also consider the CARPK dataset [43], explicitly designed for vehicle counting and used to assess cross-dataset generalization. Lastly, we critically discuss the results, highlighting the strengths and limitations of the considered methodologies, the persistent challenges in the field, and potential directions for future research.

We organize the rest of this work as follows. In Sec. II, we review the most influential surveys related to object counting,

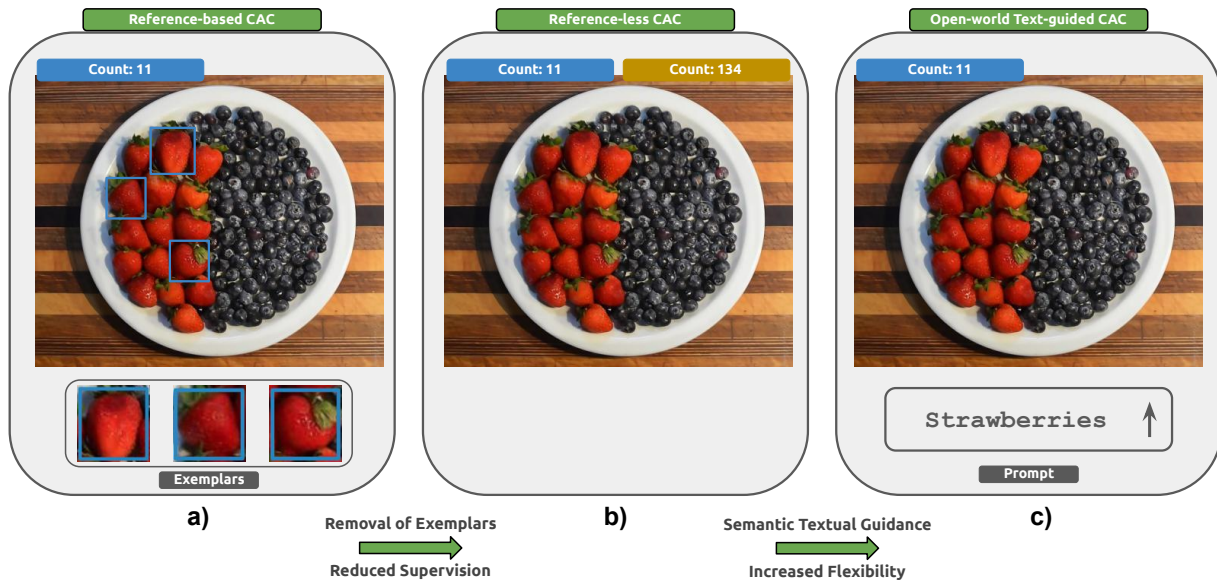


Fig. 2. **Overview of class-agnostic counting paradigms.** We propose a taxonomy to classify existing CAC methodologies: a) *Reference-based* approaches rely on annotated bounding box exemplars, which serve as visual prototypes for the object classes to be counted; b) *Reference-less* techniques relax these requirements, enabling models to automatically identify the dominant class(es) to be counted; and c) *Open-world Text-guided* methodologies allow the use of textual descriptions to specify the object classes to be considered. The arrows indicate the conceptual evolution of CAC paradigms, highlighting the progressive reduction of human supervision and the increasing flexibility and semantic control.

emphasizing the scope of the current work and outlining the search strategy. Sec. III presents the existing methods according to the taxonomy introduced earlier. Next, in Sec. IV, we provide an overview of the available datasets. In Sec. V, we present the results along with a critical discussion. Finally, in Sec. VI, we conclude the paper with insights into potential directions for future research.

II. EXISTING SURVEYS, SCOPE, AND SEARCH STRATEGY

While there are several survey papers reviewing counting methods present in the computer vision literature, most of them concentrate on specific object categories, with a particular emphasis on crowd counting. The most cited survey is [44]. In this work, Sindagi et al. revised the papers up to 2017 in detail, focusing on crowd counting and considering both traditional methodologies and techniques based on convolutional neural networks. Furthermore, they described the most used crowd counting datasets, presenting and discussing the results obtained against these benchmarks. More recently, Li et al. published a similar, more updated survey in [45], retracing the last 20 years of object counting, mainly focusing on crowd counting with density estimation using convolutional neural networks. A plethora of other surveys or short surveys have been published over the last few years: a non-exhaustive list includes [46], [47], [48], [49], [50], [51], [52], [53], [54], [55]. Even if the authors of these works look at the topic from different angles, considering various taxonomies and perspectives, they consistently focus on single-class object counting.

In contrast, our survey is the first to provide a comprehensive and structured overview of CAC methodologies. To the best of our knowledge, the only other survey that briefly

touches on CAC is [56], which covers only a few methods—likely due to the early stage of the task at the time of writing—and does not offer a systematic taxonomy or performance analysis. Conversely, our survey introduces several distinct and novel contributions: it organizes CAC methods according to an original taxonomy, systematically analyzes state-of-the-art approaches, compares their performance across benchmarks, and discusses their limitations and open challenges.

To select papers for this survey, we conducted a comprehensive search on Google Scholar for works citing FSC-147, the gold-standard benchmark introduced together with the few-shot CAC formulation by Ranjan et al. [32] (as mentioned in Sec. I). The search covered publications up to the end of 2024; the survey was completed in January 2025 before submission. Only peer-reviewed published papers were considered, excluding non-peer-reviewed preprints from arXiv unless they provided freely available implementations to ensure reproducibility.

III. EXISTING APPROACHES

In the following, we review existing methodologies by grouping them into three categories based on our proposed taxonomy: reference-based, reference-less, and open-world text-guided approaches. While some methods include additional modules or architectural tweaks that may span multiple categories, each is classified under its primary type, with cross-category features discussed where relevant. Table I summarizes the surveyed techniques, while Fig. 3 highlights key milestones over time.

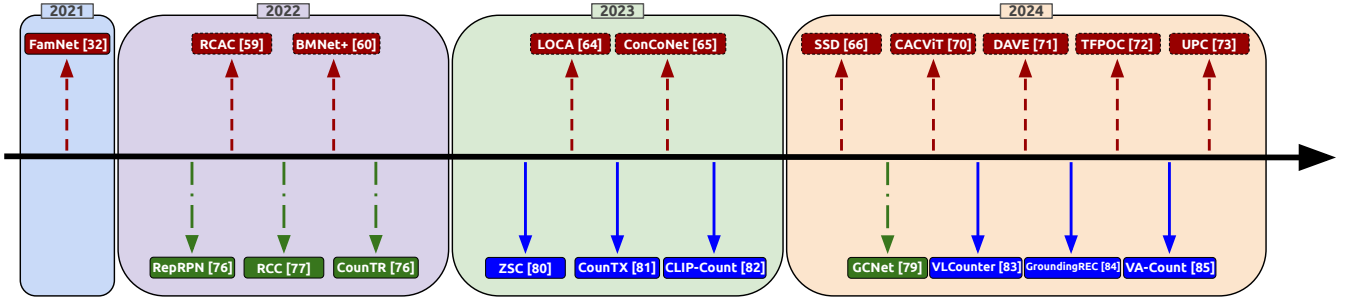


Fig. 3. **Overview of selected CAC methodologies over time.** We present a chronological overview of representative Class-Agnostic Counting (CAC) methods, highlighting milestone contributions from 2021 to 2024. Each method is encoded using both color and arrow style according to the taxonomy introduced in Fig. 2: **red** dashed arrows for *reference-based* approaches that rely on annotated exemplars; **green** dash-dot arrows for *reference-less* methods that infer dominant object classes without manual input; and **blue** solid arrows for *open-world text-guided* approaches that use natural language prompts to specify target classes. This timeline illustrates the evolution of CAC paradigms over time, showing the shift from exemplar-dependent models to more flexible and generalizable solutions.

A. Problem Formulation

State-of-the-art class-specific counting relies on supervised deep learning, typically following two strategies: detection-based and regression-based. Detection approaches identify individual instances using object detectors [25], [26], [17], [10], while regression methods estimate object counts by learning a mapping from image features to a density map [1], [20], [57], [58], whose pixel values are integrated to obtain the final count. Detectors, while conceptually simpler and capable of handling a wide range of object classes due to the abundance of suitable annotated datasets, struggle with occluded objects. This limitation is the primary reason density-based approaches have largely replaced detection-based techniques. Thus, also most class-agnostic counting techniques follow the density-based paradigm, and CAC existing benchmarks reflect this in terms of label availability. Precisely, the gold standard labels needed for the supervised training of density regressors are dots (points), i.e., ground truth corresponds to binary spatial images with 1’s at the center location of the objects, indicating their existence, and 0’s at other locations without the objects. Since directly optimizing a loss on these sparse labels is challenging, most methods generate smoothed density maps by placing Gaussian kernels G_σ at each dot location, using a fixed or adaptive σ based on object size [59], [1].

Formally, we assume to have a collection of N annotated images denoted as $\mathcal{X} = (I_1, P_1), \dots, (I_N, P_N)$, where I_i is the i -th image and $P_i \in \mathbb{R}^2$ the set of 2D point coordinates roughly localizing the objects to be counted in image I_i . The goal is to learn a regression model f_θ producing a density map $D^{map} = f_\theta(I) \in \mathbb{R}^{H \times W}$. The number of objects n in an image sub-region $S \subseteq I$ is estimated by integrating D^{map} over S , i.e., summing up pixel values in the considered region, $n = \sum_{p \in S} D_p^{map}$. The regression model is typically trained by minimizing per-pixel losses, such as the mean squared error between predicted and ground truth density maps. In the few-shot (or reference-based) counting setting, each image I_i is paired with K exemplars, defined as bounding boxes $B^E = b_{i=1:K} \in \mathbb{R}^4$ that depict instances of the target class within the same image [32], with $K = 3$ in the original formulation. Object classes are split into base C_b and novel

C_n categories, with $C_b \cap C_n = \emptyset$. For C_b , both density maps and exemplars are available; for C_n , only exemplars are provided, and the goal is to count instances by transferring knowledge from C_b (see also Fig. 4). In contrast, reference-less and text-guided zero-shot settings omit exemplars: the former automatically infers dominant class(es) via instance repetition, while the latter uses a textual description T_i to specify the target class for each image I_i .

B. Reference-based Class-agnostic Counting

a) *FamNet*: The seminal work on reference-based object counting is by Ranjan et al. [32], who first formulated counting as a few-shot regression task. Since the task was novel, the authors also introduced the first dataset tailored for it, a collection of images containing objects belonging to 147 categories named FSC-147; labels comprise dots for the training stage, and exemplar bounding boxes that are used both in the supervised learning and at inference time. See also Sec. IV for more details. Finally, the authors proposed the Few-Shot Adaptation and Matching Network (FamNet), a novel architecture designed to address this task. Specifically, it includes two main modules: (i) a multi-scale feature extraction module and (ii) a density prediction module. The first consists of the first four blocks picked up from an ImageNet pre-trained ResNet-50 backbone [89], frozen during training. The convolutional feature maps produced by the third and fourth blocks provide the representation of the images I_i ; furthermore, they are also exploited to obtain the multi-scale features of the exemplar images obtained from B^E by performing ROI pooling [90] at different scales. Rather, the density prediction module consists of some stacked convolution blocks and upsampling layers; the last one is a 1×1 convolutional layer in charge of predicting the final 2D density map D^{map} having the same size as the input image. The input of this second module does not correspond to the features produced by the feature extractor, as usual in the class-specific counting task. Instead, the authors computed the convolution operation between the scaled exemplar features and the image features, obtaining multiple correlation maps, one for each scale, that are then concatenated and fed to the density predictor. The reason

TABLE I
LIST OF THE CONSIDERED METHODS. WE SUMMARIZE THE METHODOLOGIES DISCUSSED IN THIS SURVEY, ALONG WITH SOME RELEVANT ASSOCIATED DETAILS. THE METHODS ARE CATEGORIZED BASED ON OUR PROPOSED TAXONOMY—REFERENCE-BASED, REFERENCE-LESS, AND OPEN-WORLD TEXT-GUIDED

Method	Venue	Year	Code	Pretrained Model	Point-level Supervision	Test-time Adaptation
<i>Reference-based</i>						
FamNet [32]	CVPR	2021	✓	✓	✓	✓
CFOCNet [60]	WACV	2021	✗	✗	✓	✗
VCN [61]	CVPRW	2022	✗	✗	✓	✓
RCAC [62]	ECCV	2022	✓	✗	✓	✗
BMNet+ [63]	CVPR	2022	✓	✓	✓	✗
SPDNC [64]	BMVC	2022	✓	✓	✓	✗
MACnet [65]	Pattern Recognit. Lett.	2023	✗	✗	✓	✓
SAFECount [66]	WACV	2023	✓	✓	✓	✗
LOCA [67]	ICCV	2023	✓	✓	✓	✗
ConCoNet [68]	Pattern Recognit. Lett.	2023	✗	✗	✓	✓
SSD [69]	IJCAI	2024	✓	✗	✓	✗
SATCount [70]	Neural Networks	2024	✗	✗	✓	✗
CSTrans [71]	Pattern Recognition	2024	✓	✓	✓	✗
CountVers [72]	Knowledge-Based Systems	2024	✗	✗	✓	✗
CACViT [73]	AAAI	2024	✓	✗	✓	✗
DAVE [74]	CVPR	2024	✓	✓	✓	✗
TFPOC [75]	WACV	2024	✓	✓	✗	✗
UPC [76]	AAAI	2024	✗	✗	✓	✗
PseCo [77]	CVPR	2024	✓	✓	✓	✗
CountDiff [78]	ECCV	2024	✗	✗	✓	✓
<i>Reference-less</i>						
RepRPN-Counter [79]	ACCV	2022	✓	✗	✓	N/A
RCC [80]	arXiv	2022	✓	✗	✗	N/A
CounTR [81]	BMVC	2022	✓	✗	✓	N/A
GCNet [82]	Pattern Recognition	2024	✗	✗	✗	N/A
<i>Open-world Text-guided</i>						
ZSC [83]	CVPR	2023	✓	✗	✓	✗
CounTX [84]	BMVC	2023	✓	✓	✓	✗
CLIP-Count [85]	ACM MM	2023	✓	✓	✓	✗
VLCounter [86]	AAAI	2024	✓	✓	✓	✗
GroundingREC [87]	CVPR	2024	✓	✓	✓	✗
VA-Count [88]	ECCV	2024	✓	✗	✓	✗

behind this is making the density regressor agnostic to the visual categories. During the learning stage, FamNet is trained by minimizing the mean squared error (MSE) between the predicted and the ground truth density map. Finally, this work also proposed a sort of fine-tuning that exploits test data to improve performance further. Specifically, it introduced an adaptation loss that exploits the locations of the exemplars included in the test set to be used only at inference time. It comprises two loss components: (i) the Min-Count loss, ensuring that the density sum within each exemplar box is ≥ 1 , and (ii) the perturbation loss, encouraging Gaussian-shaped density around exemplars—similar to correlation filters used in tracking [91], [92], [93].

b) CFOCNet: Roughly simultaneously, Yang et al. introduced a similar solution [60] named Class-agnostic Few-shot Object Counting Network (CFOCNet). The architecture follows the scheme of FamNet, with an encoder and decoder. The encoder includes two ResNet-50 streams for feature extraction: one for the query image and one for the exemplars

(here referred to as reference images). The features concerning the exemplars are matched by computing the convolution operation with the output of a self-attention mechanism [94] applied to the features relating to the query image. These resulting matching maps are finally fused by exploiting a scale-aware fusing mechanism, and the output is fed into the decoder to compute the density map. The decoder is similar to the one exploited in FamNet—some stacked convolution blocks and upsampling layers—and it is supervised by standard MSE loss as well as by SSIM loss [95] to catch local pattern consistency [96].

c) VCN: Some of the authors of [32] extended FamNet in [61], addressing its limitations due to the small dataset used for supervised training. They introduced the Vicinal Counting Network (VCN), which retains the core of FamNet with minor changes and incorporates a generator to augment and synthesize images from the vicinity of training samples, expanding the dataset. Specifically, the generator is fed with an input image $I \in \mathbb{R}^{H \times W \times 3}$ and a noise vector $z \in \mathbb{R}^m$,

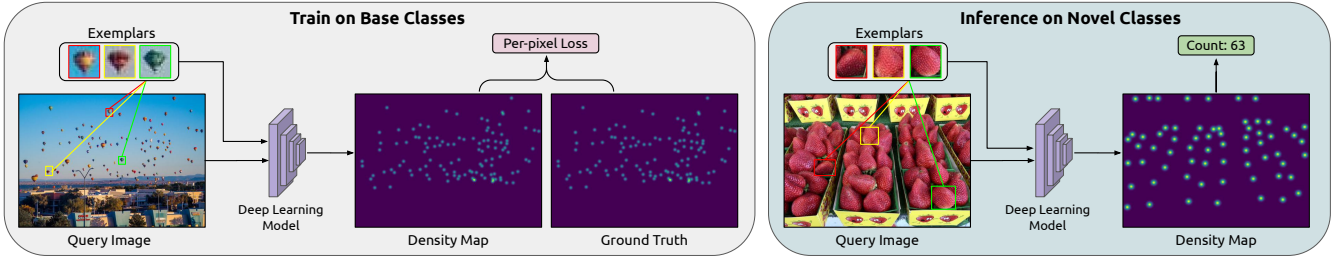


Fig. 4. **Train and inference high-level overview of reference-based CAC approaches relying on density regression.** Following the notation of this survey, CAC models are fed with query images I_i and K exemplars expressed as bounding box coordinates $B^E = \{b_i\}_{i=1:k} \in \mathbb{R}^4$. Usually, $K = 3$. Exemplars belong to several object classes, which are different at training and test time. The model is in charge of (i) computing feature representations from these inputs that should be agnostic to specific object classes, and (ii) predicting density maps D^{map} from these feature representations. Density-based methods are the standard approach for object counting in crowded scenes. Training typically involves minimizing a per-pixel loss between the predicted and ground-truth density maps, with the final count obtained by summing the pixel values of the predicted density maps.

and it produces an augmented version $I_z \in \mathbb{R}^{H \times W \times 3}$ of I . This augmented image serves as the input to the feature extractor and the subsequent regressor module, together with the original input I . The entire system is then trained jointly in a cooperative fashion. However, unlike the min-max game typical of GANs [97], VCN relies on a standard minimization problem, combining MSE loss for density regression with a reconstruction loss to enforce similarity between generated and input samples, and a diversity loss to prevent identity mapping from I to I_z . Finally, the authors used the same test time adaptation loss of FamNet [32].

d) RCAC: Another work inspired by FamNet is [62]. First, the authors explored the main limitations of FamNet by analyzing failure cases, identifying a strong dependence on exemplar diversity—exemplar boxes are few and subjectively annotated, and they may not cover all object instances or ensure intra-class diversity. To address this, they proposed the Robust Class-Agnostic Counter (RCAC), which uses a two-stream architecture: one branch processes RGB images I_i with a FamNet-like feature extractor, while the other uses a VGG-based extractor on edge images derived from I_i throughout an edge detector. This second feature extractor is randomly initialized and, different from the RGB feature extractor, optimized during training. The reason claimed by the authors behind using edge images is that edges are a sort of class-agnostic knowledge, i.e., shape is a more reliable cue across instances than color. Then, ROI pooling is applied to both branches to crop exemplar features, which are then enhanced via a feature augmentation module. After that, feature correlation is obtained by computing the convolution operation between the latter and the full feature maps, like in previous works, and the density map is predicted using the same module as in FamNet. In detail, the feature augmentation module aims to generate more exemplars of different colors, shapes, and scales in the feature space by combining the provided exemplars, sharing the goal of VCN [61] to expand the training set.

e) BMNet+: Another notable work that represents a milestone is [63]. Here, Shi et al. argued that two factors played crucial roles in previous works: (i) feature representation of query images and exemplars, and (ii) similarity metric for matching exemplar and image features. Previous methods either exploited a fixed [32], [61] or a learnable [60] feature

extractor but employed a similarity metric relying on the fixed inner product [32], [61], [60], [62], [65], which yielded insufficient matching outcomes. Hence, the authors proposed the Bilinear Matching Network (BMNet+) to improve the similarity modeling. Specifically, the authors designed a learnable bilinear similarity loss to supervise the similarity-matching results, thus going beyond the fixed inner product. The authors took inspiration from metric learning, which aims to embed data into a space where similar samples are pulled close while dissimilar ones are pushed away [98]. In more detail, their similarity loss pulls close the features between the exemplar and target instances while pushing away the features between exemplars and background patches.

f) SPDCN: Lin et al. [64] focused on the robustness of exemplar feature representations, such as in VCN [61] and RCAC [62], and proposed the Scale-Prior Deformable Convolution Network (SPDCN). The authors argued that most prior works often overlooked or poorly handled the exemplar scale during feature extraction. To address this, they leveraged size information from exemplars by exploiting scale-prior deformable convolutions [99], [100] to discard features inconsistent with scale, enabling more meaningful feature extraction. Afterward, these semantic features are split into two branches for segmentation and density estimation, respectively. In the former branch, such as in FamNet and other previous works, ROI pooling [90] is exploited to extract feature maps concerning the exemplars; next, these features are averaged into a representation vector, and a whole similarity map is calculated by computing the cosine similarity between this vector and the image feature map. In the density estimation branch, class-agnostic features are calculated using element-wise multiplication like in [32], [61], [60], [62] between the similarity map and the image feature map. Then, they are fed into a decoder that follows the design of the Pixel Shuffle Crowd Counter (PSCC) [101], which employs pixel-shuffling [102] for the upsampling operations, and that is responsible for predicting the final density map.

g) MACnet: The authors in [65] argued that bounding boxes are not the ideal representations for most exemplars as they often capture undesirable background portions that harm the matching process. Therefore, they proposed exploiting segmentation masks as an alternative, introducing the Mask

Augmented Counting network (MACnet). In more detail, the proposed architecture consists of three modules. First, an ImageNet [103] pre-trained ResNet-50 [89] is used as a feature extractor to embed both the query and the exemplars into a feature space. Specifically, its input consists of the query image I , the exemplars' bounding box coordinates B^E , and their associated masked counterparts B_m^E computed with the pre-trained Deep Extreme Cut network (DEXTR) [104]. The second module consists of a residual layer fed with the feature representation of the exemplars and their masked counterparts. Specifically, it mitigates errors during segmentation mask creation by learning from residual information instead of immediately discarding background information. Finally, the third module is responsible for predicting the density map, supervised by the MSE loss. As in previous papers [32], [60], it is fed with a similarity map obtained by convolving the feature map of the query image with the feature map resulting from the residual module as its filter, i.e., by performing the inner product between these two feature maps. However, here, the final count is derived not directly from integrating the density map but by counting the peaks utilizing a peak-finding algorithm. A final observation concerns the usage of a test time adaptation loss like in [32], [61], aiming to encourage the network in distinguishing background from foreground in the provided exemplars.

h) SAFECOUNT: You et al. introduced SAFECOUNT in [66], which uses Similarity-Aware Feature Enhancement blocks. These blocks are composed of two main modules: (i) a Similarity Comparison Module (SCM), and (ii) a Feature Enhancement Module (FEM). In SCM, query and reference features extracted by an ImageNet pre-trained ResNet-18 [89] are compared in a learnable projection space, and a score map is obtained for each reference image. The similarity map is obtained from the score map by normalizing the exemplar dimension and spatial dimension. The FEM uses the similarity map to weight the reference features, highlighting regions in the query image that are similar to the reference images. These weighted features are then fused into the query features, creating an enhanced representation that emphasizes the areas containing objects of interest.

i) LOCA: Djukic et al. focused on the strength of exemplar feature representations, arguing that, ideally, the prototypes should generalize over the appearance of the selected object category in the image. They introduced the Low-shot Object Counting network with iterative prototype Adaptation (LOCA) [67]. The core of the method is an object prototype extraction module that separately encodes shape and appearance from exemplars and refines them iteratively. Appearance is injected by initializing prototypes with RoI-pooled features from exemplar boxes over a ResNet50-based query feature map. However, this pooling makes the queries shape-agnostic, so shape information is also injected using exemplar width and height. Then, the final prototypes are obtained via an iterative adaptation module with cross-attention blocks.

j) ConCoNet: Soliven et al. introduced the Contrast Counting Network (ConCoNet) in [68]. They proposed to use not only the (positive) exemplars as in previous works but also the negative exemplars, i.e., object instances defining what

not to count. Their contribution can be incorporated into other class-agnostic counting models, and, by way of examples, they reported the results obtained using two of the milestones for the reference-based class-agnostic counting task, e.g., FamNet [32] and BMNet+ [63]. Specifically, the class-agnostic similarity maps are computed not only for the query image and positive exemplar pairs but also for the negative ones; the final similarity map input to the density regressor is obtained by simply subtracting the negative similarity map from the positive one. Since CAC datasets do not contain negative exemplars, the authors derived them under the assumption that users provide negative examples during inference, thus performing a sort of adaptation at test time; instead, to enable the training, they selected bounding boxes randomly from the query image regions classified as background by both the ground-truth and the predicted density maps.

k) SSD: Instead, in [69], the authors leveraged distinct similarity distribution characteristics between several parts of exemplar objects. They argued that different parts of an exemplar object generate distinct similarity distribution patterns. For instance, the similarity distribution at the center of the object gradually decreases from the center toward the outer regions, while the distribution at the edges varies depending on the location. To capture this, they proposed the Spatial Similarity Distribution (SSD) network, which produces a 4D similarity tensor. This allows for flexible extraction of point-to-point similarity distribution information between query and exemplar features through convolution operations in 4D space.

l) SATCOUNT: Differently, Wang et al. proposed a Scale-Aware Transformer-based class-agnostic counting framework named SATCOUNT [70]. Here, to combine the features from exemplars and the query, the authors developed a feature fusion module comprising two sub-modules: the Scale-Aware Module (SAM) and the Similarity Modeling Module (SMM). SAM combines visual and scale information to generate scale-aware visual features of exemplar objects. Meanwhile, SMM uses cross-attention to model the similarity between exemplar and query features, allowing for long-distance feature associations and the integration of global information from both exemplars and queries.

m) CSTrans: Gao and Huang [71] drew inspiration from FamNet, enhancing its architecture with two new modules: Correlation-guided Self-Activation (CSA) and Local Dependency Transformer (LDT). The resulting approach, named Correlation-guided Self-Activation Transformer (CSTrans), improves the correlation representation between the exemplar patch and query image features. Additionally, it incorporates a density map predictor based on Transformers [105] that is fully learnable and better equipped to model local context dependencies.

n) CountVers: The authors in [72] focused on a novel correlation mechanism between exemplar-query features, overcoming the limitations of kernel-wise convolution characterizing previous works such as FamNet. Specifically, they proposed CountVers, which integrates both channel-wise and spatial-wise correlation to handle small and large object counting. The method builds on two insights: small objects have localized features, making channel-wise correlation beneficial,

while large objects span broader regions with complex spatial semantics, requiring spatial-wise correlation for accurate counting.

o) CACViT: Recently, Zhicheng et al. [73] introduced a framework based on a pre-trained Vision Transformer (ViT) and an "extract-and-match" paradigm that removes the need for multiple feature extractors or post-processing. The attention mechanism in ViT is shown to handle both feature extraction and matching by processing concatenated query and exemplar tokens. Within the ViT, self-attention extracts features from both inputs, while cross-attention enables matching between them.

p) DAVE: Pelhan et al. recently introduced a detect-and-verify paradigm (DAVE) [74] that combines the strengths of density-based methods—best suited for crowded scenarios—with those of detection-based techniques, which provide precise object localization. This approach follows a two-stage pipeline. In the first detection stage, DAVE generates a high-recall set of candidate bounding boxes by first estimating the object centers through a location density map and then predicting bounding box parameters using a regression head. The verification stage refines these detections by removing false positives. Each candidate is analyzed based on its appearance features, which are compared to features of the provided exemplars using clustering methods. Detections that do not align with exemplar clusters are classified as outliers and removed. The refined bounding boxes are then used to update the density map, which further improves count estimation accuracy.

q) TFPOC: Different from the above-described architectures, TFPOC [75] employed a detection-based technique, leveraging the popular Segment Anything Model [106] for instance segmentation that does not require additional training or fine-tuning for class-agnostic counting. Initially, the authors presented a baseline method. This involves generating binary masks for reference objects using input prompts such as points or boxes, computing a similarity map between the image features and reference object features via cosine similarity, and producing masks for all objects in the image using a grid of point prompts. Target objects are identified by calculating similarity scores for each mask and applying a threshold to determine relevance. The final count is obtained by summing the identified target objects. However, this vanilla approach is computationally intensive as it processes all objects in the image and struggles with setting an optimal similarity threshold, which can lead to undercounting or overcounting. To address these limitations, the authors proposed an advanced prior-guided mask generation method, enhancing the segmentation process with three types of priors. The similarity prior uses a binarized similarity map to guide the segmentation model in focusing on target regions. The segment prior prevents redundant processing by maintaining an overall segment map and refining segmentation iteratively. The semantic prior incorporates reference object features to better guide the mask decoder in identifying and segmenting the target objects.

r) UPC: A token-based framework for unified open-world text-guided counting (UPC) is introduced in [76]. Prompts, which may take the form of boxes, points, or text,

are first transformed into a unified representation called a prompt mask. For box and point prompts, this mask is derived directly from the labeled regions or pixels within the image. As in previous methods, image features are extracted using a CNN-based encoder, and a cross-attention mechanism is applied to determine the similarity between the prompt token and the image features. This similarity guides the creation of density features, which are subsequently decoded by a CNN to produce the final density map. However, in this work, to improve the robustness of the model, the predicted density map is iteratively refined by reusing it as a new prompt mask, leading to convergence toward consistent outputs. A fixed-point loss function, based on implicit differentiation, stabilizes training and improves parameter optimization. Additionally, a contrastive training strategy is used: positive samples contain objects matching the prompt, while negative ones do not. This forces the model to produce accurate density maps for positives and zero-density maps for negatives, reducing errors from noisy or ambiguous prompts.

s) PseCo: As in TFPOC [75], the authors in [77] exploited a detection-based approach relying on the popular SAM [106] for instance segmentation. Specifically, they introduced a framework termed Point, Segment and Count (PseCo). Different from TFPOC, PseCo does not use uniform grid points to prompt SAM to segment all objects. Indeed, the authors argued that using grid points may fall short in capturing all objects, particularly in densely crowded scenes, leading to the omission of many small objects. Although increasing the density of grid points could help address this limitation, it would result in substantial computational overhead. Thus, a class-agnostic object localization method was proposed in [77], estimating a heatmap from which object coordinates are inferred and used to guide SAM. Then introduced a second stage that integrates another foundation model, the Contrastive Language–Image Pretraining (CLIP) model [107], to classify regions identified in the first stage based on given exemplars.

t) CountDiff: Hui et al. [78] proposed CountDiff, a framework designed to boost CAC by leveraging knowledge from a pre-trained diffusion model. To encode exemplar-specific information, CountDiff learns an object-specific embedding by mapping image features into the text embedding space, enabling the diffusion model to interpret the visual characteristics of the target object. To enhance generalization in CAC, CountDiff complements this with an object-agnostic embedding, capturing transferable knowledge from the diffusion model's cross-attention layers. By combining both embeddings, the framework effectively exploits cross-attention maps to identify regions relevant for CAC. Finally, a lightweight test-time adaptation step fine-tunes the object-specific embedding using the provided exemplars, further boosting accuracy on novel objects.

C. Reference-less Class-agnostic Counting

a) RepRPN-Counter: The first reference-less class-agnostic counting method was introduced in [79]. In this paper, Ranjan et al. introduced the Repetitive Region Proposal Network Counter (RepRPN-Counter), which predicts

separate density maps for each repetitive object category in a given query image. The model is based on FamNet [32] and includes an upstream module called the Repetitive Region Proposal Network (RepRPN), designed to automatically identify exemplars of repetitive objects in the image, which are then passed to FamNet for further processing. RepRPN takes inspiration from the Region Proposal Network (RPN) of the popular Faster R-CNN object detector [108]. RPN typically calculates proposal boxes and objectness scores, but RepRPN additionally outputs a so-called repetition score, indicating how frequently an object within the proposals appears in the image. These repetition scores are used to select exemplars from the repetitive object categories in the query image, with the highest-scoring proposals chosen as exemplars. A key challenge in training RepRPN was the lack of labels in class-agnostic counting datasets like FSC-147 [32], where annotations are provided for only one object category, despite the presence of other unannotated objects (see also Sec. IV). Penalizing predictions for these unlabeled objects could harm performance. To overcome this, the authors used knowledge transfer: RepRPN trained on MSCOCO [109] acted as a teacher to assign objectness and repetition scores to proposals not overlapping with annotated objects, while a pre-trained FamNet generated density maps for these proposals using single exemplars.

b) RCC: [80] went a step further by proposing RCC - Reference-less class-agnostic counting. Unlike previous works, it did not use point-level supervision—besides not using any exemplars as in the reference-less setting—thus proposing a weakly-supervised methodology. Specifically, their proposed network directly regresses to a single scalar count prediction for the entire input image, thus not requiring ground-truth density maps for supervised learning. To create a general and informative feature space without labels, the authors implemented a self-supervised knowledge distillation technique based on [110]. They encouraged the learning of meaningful image representations by fostering agreement between a fixed teacher network, which processes large global image crops, and a student network, which analyzes smaller local image crops. This alignment is achieved by minimizing the cross-entropy between the probability distributions produced by both networks.

c) CounTR: Another milestone concerning reference-less class-agnostic counting is represented by Counting TRansformer - CounTR [81] (pronounced "counter"). In this work, Liu et al. built on the idea that self-similarity serves as a strong prior in visual object counting. They introduced a transformer-based architecture where self-similarity can be explicitly captured by the inherent attention mechanisms, both between input image patches and with the exemplars (if any). Specifically, this architecture features two visual encoders: (i) a Video Transformer (ViT) [111], which maps input image features into a high-dimensional feature space, and (ii) a lightweight CNN, responsible for extracting visual features from the exemplars (if available). The subsequent feature interaction module is responsible for merging information from both encoders. It consists of a series of standard transformer decoder layers, where the image features serve as the *Query*,

and two separate linear projections of the exemplar features, or a learnable special token if no exemplars are present, act as the *Key* and *Value*. This architecture aligns well with the self-similarity prior in counting tasks: self-attention captures similarities between image regions, while the cross-attention between *Query* and *Value* compares these regions with the exemplars or learns to bypass the CNN branch when using the learnable token, i.e., in the reference-less setting where no exemplars are provided. Additionally, the authors proposed a two-stage training approach, where the transformer-based image encoder is first pre-trained using self-supervision through masked image modeling [112], followed by supervised fine-tuning for the counting task.

d) GCNet: Also the authors of [82] introduced a technique that does not use point-level supervision such as [80], named GCNet - Generalized Counting Network. However, differently from [80], GCNet uses a pseudo-Siamese structure to capture pseudo-exemplar cues from the resized raw image. Specifically, the main branch of the network extracts primary 2D feature maps from an input image I_i . In contrast, the secondary branch is in charge of generating exemplar-focused outputs by exploiting a methodology inspired by vision transformers [111]. The output of the main branch is then further processed through an anisotropic encoder to capture discriminative features along three directions in feature space—horizontal, vertical, and basis/channel directions. Finally, these two outputs are fed into a dual-attention condenser. The same authors also proposed a reference-based version of GCNet, which attaches an additional ResNet-50 backbone to the front-end of the original GCNet for processing labeled exemplar patches; the exemplar features are then fed into the same back-end structure of GCNet to predict an auxiliary single count.

e) Adaptations: Some existing reference-based techniques have been adapted to the reference-less setting. Specifically, some minor modifications have been implemented to the module of LOCA [67] in charge of extracting object prototypes. Moreover, the authors of DAVE [74] made adjustments to their architecture, replacing the location density prediction component with a reference-less version of LOCA. However, the detection stage and most of the verification stage remained unchanged. The only alteration in the verification stage involves the cluster selection process: clusters with a size of at least 45% of the largest cluster are retained as positive detections, while the others are classified as outliers. This adjustment addresses potential cluster fragmentation due to the lack of exemplars that define appearance similarity levels. Lastly, the authors of [79] proposed a modified version of FamNet, incorporating a standard Region Proposal Network (RPN) from the widely used Faster R-CNN object detector [108] for exemplar generation.

D. Open-world Text-guided Object Counting

a) ZSC: Xu et al. [83] were the first to propose an open-world text-guided approach, introducing a more versatile paradigm called zero-shot counting (ZSC) where users can specify textual descriptions of the object classes they want to

count, representing a sort of trade-off between previous class-agnostic counting paradigms—humans are still in the loop but can specify classes with less effort and in a more natural way. In more detail, their proposal is grounded on an effective strategy for selecting meaningful patches from the input image that contain the target object specified by a class name, to be used as exemplars. To this end, they construct a class prototype in a pre-trained embedding space using the provided class name, and then select patches whose embeddings are among the k -nearest neighbors to that prototype. This is implemented using a conditional variational autoencoder (VAE) built on the widely adopted Contrastive Language-Image Pretraining (CLIP) model [107], which generates visual exemplar prototypes conditioned on the semantic embedding of the given category name.

b) CounTX: Concurrently, Amini-Naieni et al. [84] proposed an alternative solution called CounTX (pronounced "Count-text"). CounTX can be trained end-to-end and accepts more detailed specifications of target objects for counting, rather than relying solely on class names. To support this, the authors introduced an enhanced version of the FSC-147 dataset [32], named FSC-147-D, where object classes are described using more fine-grained and structured natural language sentences (See also Sec. IV for more details). Specifically, CounTX extends the reference-less CounTR architecture [81] to the open-world text-guided setting. Like CounTR, it features a transformer-based image encoder, but it utilizes the CLIP vision transformer B-16 [107], pre-trained in a contrastive manner with a transformer-based text encoder using image-text pairs from LAION-2B [113]. In more detail, the image encoder encodes each input image into a spatial map of 512-dimensional feature vectors, while the text encoder processes the class description into a single 512-dimensional feature vector. To combine these features, the authors employed a transformer-based feature interaction module, similar to CounTR, but instead of matching image patches to visual exemplars, in CounTX, it is exploited to compute the similarities between image patches and class descriptions. Finally, the output of the feature interaction module is reshaped to a spatial feature map and fed into a progressive four-block convolution and upsampling operation to produce density maps.

c) CLIP-Count: CLIP-Count [85] is another method built on the Contrastive Language-Image Pretraining (CLIP) model [107], designed to align text embeddings with dense visual features. In this approach, text embeddings are compared with image patch embeddings. Key features of this method include: (i) the use of an InfoNCE-based contrastive loss [114], commonly employed in contrastive learning to encourage meaningful and discriminative representations by pulling similar data points (positive pairs) closer in the latent space and pushing dissimilar ones (negative pairs) further apart. This loss is used alongside the classic MSE loss, applied to binary ground-truth masks that distinguish between positive and negative patch regions; and (ii) a hierarchical patch-text interaction module that propagates semantic information across different resolution levels of visual features. For density map generation, the decoder employs a conventional design based on convolutional and upsampling layers.

d) VLCounter: In [86], the authors incorporated three modules to efficiently fine-tune CLIP for the counting task and to exploit intermediate features across different encoding layers of CLIP in the decoding stage. In particular: (i) a semantic-conditioned prompt-tuning module is responsible for fine-tuning CLIP efficiently, using conditioning via semantic embeddings to generate patch embeddings that highlight the region of interest, rather than relying on simple learnable prompts; (ii) a learnable affine transformation module adjusts the semantic-patch similarity map produced by the previous module to better suit the counting task; (iii) a segment-aware skip connections module is utilized to capture intermediate features from various encoding layers of CLIP, enhancing the generalization ability of the decoder and providing rich contextual information.

e) GroundingREC: [87] addressed a key limitation in object counting, which is often restricted to class-level granularity and overlooks fine-grained distinctions. However, in real-world scenarios, counting typically requires contextual or referential input—for example, distinguishing traffic flow directions or separating stationary from moving pedestrians and vehicles at a junction. To tackle this, the authors introduced a novel task called Referring Expression Counting (REC), which focuses on counting objects with distinct attributes within the same class. To evaluate the REC task, they developed a new dataset named REC-8K, comprising 8011 images and 17,122 referring expressions (See also Sec. IV for more details). The methodology leverages the open-set detector GroundingDino [115], adapted with specific modifications such as replacing bounding boxes with box centers and utilizing the CLS token as a representation of the global semantics of the referring expression (rather than individual text tokens). In addition to REC, they also evaluated their method on class-agnostic counting, demonstrating its generalizability to prior tasks.

f) VA-Count: In [88], the authors addressed the challenge of identifying high-quality exemplars for zero-shot counting, introducing the Visual Association-based Zero-shot Object Counting (VA-Count) framework. VA-Count includes two main components: the Exemplar Enhancement Module (EEM) and the Noise Suppression Module (NSM), which respectively refine exemplar selection and mitigate the impact of incorrect samples. The EEM leverages GroundingDino [115], as in [87], but adds a binary filter to select candidate exemplars containing exactly one object. Despite this, errors may occur when selected exemplars do not belong to the target category. The NSM addresses this by identifying and filtering out such negative exemplars. Using contrastive learning, it distinguishes between relevant and irrelevant samples, enhancing the robustness of the counting process.

g) Adaptations: Some reference-based techniques have been adapted for the open-world text-guided setting. For example, the authors of DAVE [74] introduced minor adjustments to their architecture, particularly in the cluster selection process during the verification stage. In this approach, the text prompt embedding is derived using the CLIP model [107] and compared to the CLIP embeddings of the identified clusters. Cluster embeddings are computed by masking out

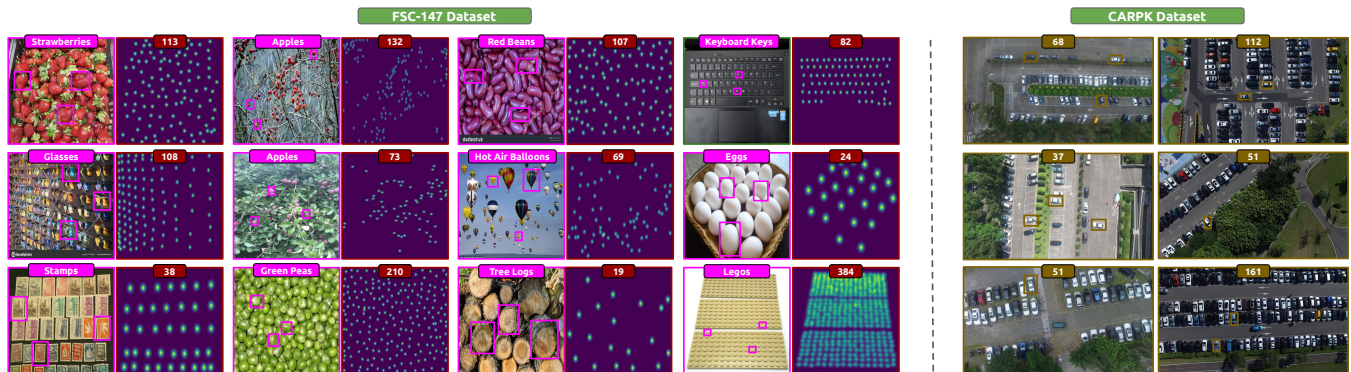


Fig. 5. **Dataset samples.** We show some samples from the CAC gold standard benchmarks, together with bounding boxes marking the exemplars. (a) The FSC-147 dataset [32] includes more than 6,000 images belonging to 147 object classes. We present sample images along with the provided labels, which include density maps and three bounding boxes localizing the exemplars. (b) The CARPK dataset [43], a collection of drone-view images tailored for vehicle counting, which is often used to assess cross-dataset generalization capabilities on the specific *vehicle* category. We show sample images together with 12 bounding boxes marking the exemplars (as set by [32]).

image regions outside the bounding boxes associated with each cluster and then obtaining the CLIP embedding for the remaining regions. Cosine distances are calculated between the text embedding and each cluster embedding, and clusters with less than 85% of the highest prompt-to-cluster similarity score are classified as outliers. Similarly, the authors of TFPOC [75] enabled textual inputs to define object classes. Their method begins with a coarse similarity map generated using CLIP-Surgery [116], an enhanced variant of CLIP. From this map, reference objects are identified through a series of steps: the similarity map is binarized, the largest connected component (likely containing the target objects) is isolated, and bounding boxes are created around sub-regions within this component for further refinement. These bounding boxes are then used as prompts for Segment Anything Model [106], producing a high-quality similarity map. In another approach, the authors of [76] employed CLIP to generate a prompt mask inspired by MaskCLIP [117]. Cosine distance was utilized to compute the matching score between predefined text features and the corresponding visual features. In PseCo [77], similar to the few-shot setting, the authors used the CLIP text embeddings as classification weights when only known class names. Finally, CountDiff [78] can be straightforwardly switched to perform open-world text-guided CAC by obtaining the object-specific embedding leveraging the pre-trained text encoder in the text-to-image diffusion model

IV. DATASETS

There is a lack of publicly available data for the CAC task. Indeed, most existing counting datasets are designed for specific object categories. Notable examples include UCF-QNRF [118], ShanghaiTech [59], and WorldExpo’10 [4] for crowd counting; TRANCOS [119] and NDISPark [41], [120] for vehicle counting; Pest Sticky Traps [18], [121] for pest abundance estimation; and VGG Cell [31] for cell estimation. Meanwhile, datasets that include multiple object categories, such as the MSCOCO dataset [109], are unsuitable for counting tasks because they were designed for object detection, typically featuring images with only a small number of object

instances. In this section, we outline the limited CAC benchmarks available in the literature. Among them, FSC-147 [32] is considered the gold standard. Additionally, although originally intended for vehicle counting, CARPK [43] is widely used to evaluate generalization capabilities. Fig. 5 illustrates some samples from these two latter benchmarks.

a) *FSC-147*: The FSC-147 dataset comprises 6,135 images spanning 147 object categories, including plants, animals, vehicles, and food. Annotations were manually created by marking dots over the approximate centroids of each object instance—as usual for the object counting task [1]. Additionally, the dataset includes the coordinates of three bounding boxes per image, representing exemplar instances. Each image contains exemplars belonging to a single category, whose natural language name is stored in a text file. If multiple categories were present in an image, one was chosen arbitrarily. Another characteristic of FSC-147 is the significant variation in object counts per image, ranging from 7 to 3,731, with an average of 56 objects per image. The dataset is divided into three splits: 89 object categories are allocated to the training set, while 29 categories are assigned to the validation and testing sets. These splits consist of 3,659, 1,286, and 1,190 images, respectively.

b) *FSC-133*: A revised version of FSC-147, called FSC-133, was introduced in [80]. The authors identified and corrected several errors in FSC-147. Specifically, they found that (i) 11 training images also appeared in validation or test sets, (ii) some images were near-duplicates with pixel-wise differences close to zero, and (iii) certain duplicates had inconsistent ground truth counts, with discrepancies up to 25%. To address these issues, FSC-133 merged very similar categories and retained only the images with the most accurate counts. The revised dataset consists of 5,898 images across 133 categories, with splits containing 3,877 images for training, 954 for validation, and 1,067 for testing. However, despite the improvements introduced with FSC-133, subsequent works have largely continued to use FSC-147, which remains the standard for this task.

c) *FSC-147-D and REC-8K*: Another enhanced version of FSC-147, called FSC-147-D, was introduced by [84] to

better support the open-world text-guided object counting paradigm. In this version, Amini-Naieni et al. replaced the simpler object descriptions with more fine-grained and structured natural language sentences for each image, specifying the objects to be counted with greater precision. In a similar direction, REC-8K [87] is a collection of approximately 8,000 images drawn from existing datasets, including FSC-147, where the textual descriptions of object categories are enriched with attributes.

d) *OmniCount-191 and MCAC*: Moreover, two datasets have addressed a key limitation of FSC-147—its limited number of images featuring multiple object categories—by including images with multiple categories: OmniCount-191 [122] and MCAC [123]. However, both present significant drawbacks. OmniCount-191 contains a low number of objects per image, and many images within the same category are visually similar—often being augmented versions of the same source—even across training and test splits. MCAC, on the other hand, is synthetic and lacks appropriate annotations for open-world text-guided approaches, limiting its applicability to realistic scenarios. Notably, still within the context of synthetic data, [124] and [125] proposed approaches relying on text-to-image latent diffusion models to produce counting data across diverse object categories.

e) *CARPK*: Finally, several existing papers have also evaluated their performance on the CARPK dataset [43], a collection of drone-view images of parking lots specifically designed for vehicle counting. This benchmark was first utilized for CAC by the work that introduced FSC-147 and has since been used by subsequent works, primarily to assess cross-dataset generalization on the specific *vehicle* category. The dataset comprises 1,448 images, divided into a training set of 989 images and a test set of 459 images, with approximately 90,000 annotated vehicles in total. In CAC, this dataset is used either without any annotations or with a set of 12 randomly selected exemplars.

V. RESULTS AND DISCUSSION

In this section, we present the results of the evaluated methods, following the same taxonomy of previous sections—reference-based, reference-less, and open-world text-guided approaches. First, we describe the experimental setting and then provide a critical analysis of the outcomes across various points of discussion.

A. Experimental Setting

Some techniques have been adapted to carry out more than one of these tasks (see also Sec. III); in these cases, we report the results for all of them. We considered the two most commonly used benchmarks: FSC-147 [32] and CARPK [43]. For FSC-147, in line with existing literature, we report results for both the validation and test subsets. Differently, the CARPK dataset is used to evaluate the generalization capabilities of the models in counting instances of a specific object class—vehicles. Previous works have explored two different settings: i) training models on FSC-147 without using any data from CARPK nor the car category in FSC-147, and ii) fine-tuning

models using training data from CARPK, where a set of 12 exemplars is randomly sampled from the training set and used as exemplars across all training and test images.

We show the outcomes in terms of two popular counting metrics, following previous literature, i.e., using the mean absolute error (MAE) and the root mean squared error (RMSE), defined as $MAE = \frac{1}{N_T} \sum_{n=1}^{N_T} |\tilde{c}_n - c_n|$ and $RMSE = \sqrt{\frac{1}{N_T} \sum_{n=1}^{N_T} (\tilde{c}_n - c_n)^2}$, where N_T is the number of test images, and \tilde{c}_n and c_n are the ground truth and predicted counts, respectively.

B. Reference-based Results

Table II shows the results achieved by the surveyed reference-based methods on FSC-147. We also report the results concerning two trivial baselines, as in [32], i.e., always output the average object count for training images and always output the median count for training images.

The pioneering FamNet [32] laid the groundwork for this paradigm with an MAE and an RMSE of 22.08 and 99.54 on the test subset. Subsequent works progressively improve the performance, sometimes revising and adapting this foundation model. For instance, VCN [61], RCAC [62], and SPDCN [64] focused on the robustness of exemplar feature representations, improving generalization, and highlighting the importance of robust training data diversity. Especially, VCN and SPDCN reached an impressive MAE of 18.17 and 13.51, respectively. Differently, MACnet introduced segmentation masks as an alternative to bounding boxes for exemplar representation, demonstrating that finer object delineation can improve model robustness. The subsequent method that has marked a breakthrough is BMNet+, which was one of the first works that improved the matching technique between image and exemplar features, moving away from the naive idea of the fixed inner product between them. SAFECount [66] also followed the direction of improving the image-exemplars matching mechanism and achieved an MAE and RMSE of 14.32 and 85.54, respectively (again, on the test subset). Other methods that stood out are SSD [69], LOCA [67], and CACViT [73], which sensibly lowered both MAE and RMSE. The latter approach proposed a particularly interesting "extract-and-match" paradigm, which basically totally relies on the attention mechanism of Video Transformer [111]. Additionally, ConCoNet is worth mentioning since it proposed a training strategy potentially applicable to all the other methods that brought the idea of leveraging negative exemplars to better distinguish between target and background regions. However, the model achieving state-of-the-art results is DAVE [74]. By employing a detect-and-verify strategy, DAVE combines bounding-box detection with clustering-based verification to eliminate outliers effectively. On the leaderboard, DAVE demonstrates the lowest MAE and RMSE values to date (8.66 and 32.36, respectively, on the test subset), showcasing its dominance in the reference-based paradigm. This performance leap is not solely due to architectural complexity but reflects a shift in design philosophy. Earlier regression-based methods like FamNet are vulnerable to background clutter, which can produce false density peaks and catastrophic counting errors. DAVE addresses this by

TABLE II
RESULTS ON THE FSC-147 DATASET [32]. WE REPORT THE PERFORMANCE IN TERMS OF MAE AND RMSE REACHED BY THE METHODOLOGIES
 DISCUSSED IN THIS SURVEY OVER THE GOLD STANDARD CAC BENCHMARK—FSC-147. THE BEST RESULTS ARE IN BOLD.

Method	Val Set		Test Set	
	MAE ↓	RMSE ↓	MAE ↓	RMSE ↓
<i>Baseline</i>				
Mean	53.38	124.53	47.55	147.67
Median	48.68	129.70	47.73	152.46
<i>Reference-based (3 exemplars)</i>				
FamNet [32]	23.75	69.07	22.08	99.54
CFOCNet* [60]	21.19	61.41	22.10	112.71
VCN [61]	19.38	60.15	18.17	95.60
RCAC [62]	20.54	60.78	20.21	81.86
BMNet+ [63]	15.74	58.53	14.62	91.83
SPDCN [64]	14.59	49.97	13.51	96.80
MACnet [65]	20.65	-	18.38	-
SAFECount [66]	15.28	47.20	14.32	85.54
LOCA [67]	10.24	32.56	10.79	56.97
ConCoNet (FamNet) [68]	18.77	58.96	18.02	91.63
ConCoNet (BMNet) [68]	15.03	57.94	14.21	91.12
SSD [69]	9.73	29.72	9.58	64.13
SATCount [70]	12.27	45.91	10.77	61.14
CSTrans [71]	18.10	58.45	16.38	93.51
CountVers [72]	11.45	42.29	11.28	90.10
CACViT [73]	10.63	37.95	9.13	48.96
DAVE [74]	8.91	28.08	8.66	32.36
TFPOC [75]	-	-	19.95	132.16
UPC [76]	16.87	59.45	16.68	105.08
PseCo [77]	15.31	68.34	13.05	112.86
CountDiff [78]	8.43	31.03	9.24	53.41
CounTR ^{\$} [81]	13.13	49.83	11.95	91.23
GCNet ^{\$} [82]	19.61	66.22	17.86	106.98
<i>Reference-less</i>				
RepRPN-Counter (Top5) [79]	29.24	98.11	26.66	129.11
RCC [80]	17.49	58.81	17.12	104.53
CounTR [81]	17.40	70.33	14.12	108.01
GCNet [82]	19.50	63.13	17.83	102.89
FamNet (Top5) ^{\$\$†} [32]	32.15	98.75	32.27	131.46
LOCA ^{\$\$} [67]	17.43	54.96	16.22	103.96
DAVE ^{\$\$} [74]	15.54	52.67	15.14	103.49
<i>Open-world Text-guided</i>				
ZSC [83]	26.93	88.63	22.09	115.17
CounTX** [84]	17.70	63.61	15.73	106.88
CLIP-Count [85]	18.79	61.18	17.78	106.62
VLCOUNTER [86]	18.06	65.13	17.05	106.16
GroundingREC ⁺⁺ [87]	10.06	58.62	10.12	107.19
VA-Count [88]	17.87	73.22	17.88	129.31
DAVE [‡] [74]	15.48	52.57	14.90	103.42
TFPOC ^{‡+} [75]	47.21	127	24.79	137.15
UPC [76] [‡]	16.92	58.92	16.81	105.83
PseCo [77] [‡]	23.90	100.33	16.58	129.77
CountDiff [78] [‡]	15.50	54.33	14.83	103.15

* re-implemented by [63]; \$ reference-based modification of a reference-less method; \$\$ reference-less modification of a reference-based method; † implemented by [79]; ‡ prompt-based modification of a reference-based method; + results on the validation set computed by [87]; ** trained on the FSC-147-D dataset [84]; ++ trained on the REC-8K dataset [87].

decoupling the process: first generating candidate detections, then verifying them against exemplar clusters. This verification stage acts as a semantic filter, rejecting outliers and enforcing consistency with the exemplar distribution. Finally, it is worth noting that the best MAE on the validation subset is achieved by CountDiff [78]. However, this result relies on a test-time adaptation strategy, making the comparison not entirely fair since additional training occurs during inference. Without this component, performance is less competitive—MAE/RMSE of 9.15/31.97 on the validation subset and 9.97/54.89 on the test subset.

C. Reference-less Results

In Tab. II, we report the results obtained by the surveyed reference-less approaches on FSC-147. The first reference-less approach, RepRPN-Counter [79], introduced the concept of repetitive region proposals and reached an MAE of 26.66 and an RMSE of 129.11 on the test subset. These error metrics are significantly higher than those obtained with reference-based approaches, as expected, since reference-less techniques do not utilize bounding box exemplar annotations. Subsequent methods have significantly improved performance. CounTR [81], a transformer-based reference-less framework, leverages the self-similarity of image regions and achieves competitive results, with an MAE of 14.12 and an RMSE of 108.01 on the test subset. Another notable contribution is RCC [80]. Besides achieving competitive results (an MAE of 17.12 and an RMSE of 104.53), it employs a weakly supervised learning approach that does not need point-level annotations, thereby representing a particularly interesting approach in data scarcity scenarios. In the same direction, also GCNet [82] does not use dot labels and obtained comparable results to RCC. Overall, there is no clear winner in this leaderboard. Indeed, on the one hand, the reference-less version of DAVE [74] achieves the best results in the validation split with an MAE and RMSE of 15.54 and 52.67, respectively; on the other hand, CounTR and GCNet shine in the test subset with an MAE of 14.12 and an RMSE of 102.89.

These results highlight a key trade-off in reference-less CAC: while these methods eliminate the need for exemplar annotations and offer greater flexibility, they often suffer from semantic ambiguity and background clutter. Without explicit guidance, they rely on visual repetition to infer the dominant object class, which can lead to false positives in complex scenes.

D. Open-world Text-guided Results

In the last part of Tab. II, we show the results concerning the considered open-world text-guided approaches, which represent a recent and promising advancement in class-agnostic counting, driven by the progress of large multi-modal models. However, similar to the reference-less case, this flexibility comes at the expense of lower performance compared to reference-based techniques. The first milestone, ZSC [83], obtained an MAE and an RMSE of 22.09 and 115.17 on the test subset. Among the subsequent methods that steadily improved performance, CounTX [84] emerges as a particularly

competitive approach, in some way adapting its counterpart CounTR [81] to this new setting. It achieves an impressive MAE of 15.73 and an RMSE of 106.88 on the test subset. However, the best results were contended by two open-world text-guided variants of reference-based methods—DAVE [74] and CountDiff [78]—and GroundingREC [87]. The first two excel in RMSE, indicating greater robustness to outliers, while GroundingREC achieves the best MAE (10.06 and 10.12 on the validation and test subsets, respectively).

Beyond raw performance dictated by architectural choices, the effectiveness of text-guided counting is also influenced by the richness of the textual prompts used. While most methods rely on simple class names, recent approaches have explored more structured and semantically expressive prompts. For instance, CounTX is trained on the FSC-147-D dataset, which replaces basic labels with more descriptive textual sentences. Similarly, GroundingREC is trained on the REC-8K dataset, where prompts include object attributes. Notably, both CounTX and GroundingREC rank among the top-performing models in our evaluation, suggesting that richer prompts can lead to more accurate and robust counting. These results highlight the potential of moving beyond minimal textual input toward more informative and context-aware prompting. Future research could explore automatic prompt generation, adaptive refinement mechanisms, and multimodal reasoning strategies to further improve semantic alignment and generalization in open-world scenarios, possibly also considering the contextual capabilities of large multimodal models as part of broader reasoning pipelines.

E. Trade-offs Between Guidance and Accuracy

A central theme emerging from these results is the fundamental trade-off between performance and convenience across the three CAC paradigms. While reference-based methods consistently achieve the best results (e.g., DAVE [74] achieves an MAE of 8.66 on FSC-147 test set), they require human-annotated exemplars at inference time, limiting scalability and automation. In contrast, reference-less and open-world text-guided approaches offer greater convenience—eliminating or automating the need for exemplars—but at a measurable cost in accuracy. This “price of convenience” is starkly illustrated by the more than 70% increase in MAE observed when moving from DAVE (8.66) to its reference-less variant (15.14) or its open-world text-guided version (14.90).

However, beyond the illustrative case of DAVE, all reference-less and open-world text-guided approaches consistently show lower performance compared to reference-based techniques. Notably, the RMSE is particularly affected by the change of paradigm: the best results on the FSC-147 test set are achieved by DAVE with an RMSE of 32.36, GCNet [82] with 102.89, and the text-guided version of DAVE with 103.42, representing the top-performing models in the reference-based, reference-less, and text-guided paradigms, respectively. We argue that this large error gap in RMSE can often be attributed to the use of poor-quality or even incorrect exemplars—a challenge that becomes more pronounced in the absence of reference bounding boxes—and may result in catastrophic

TABLE III
RESULTS ON THE CARPK DATASET [43]. WE REPORT THE PERFORMANCE IN TERMS OF MAE AND RMSE OBTAINED WITH SOME OF THE METHODOLOGIES DISCUSSED IN THIS SURVEY OVER THE CARPK BENCHMARK. FOLLOWING PREVIOUS LITERATURE, CARPK IS EXPLOITED FOR TESTING CROSS-DATASET GENERALIZATION OVER A SPECIFIC OBJECT CLASS—VEHICLES. THE BEST RESULTS ARE IN BOLD.

Method	Fine-Tuned	MAE ↓	RMSE ↓
<i>Baseline</i>			
Mean	N/A	65.63	72.26
Median	N/A	67.88	74.58
<i>Reference-based (12 exemplars)</i>			
FamNet [32]	✓	18.19	33.66
RCAC [62]	✓	13.62	19.08
BMNet+ [63]	✓	5.76	7.83
SPDCN [64]	✓	10.07	14.12
SAFECount [66]	✓	5.33	7.04
CSTrans [71]	✓	5.06	6.53
CountVers [72]	✓	5.19	6.55
CACViT [73]	✓	4.91	6.49

FamNet [32]	✗	28.84	44.47
RCAC [62]	✗	17.98	24.21
BMNet+ [63]	✗	10.44	13.77
SPDCN [64]	✗	18.15	21.61
ConCoNet (FamNet) [68]	✗	23.55	32.41
ConCoNet (BMNet) [68]	✗	16.40	21.54
SAFECount [66]	✗	16.66	24.08
LOCA [67]	✗	9.97	12.51
SATCount [70]	✗	9.51	12.67
CACViT [73]	✗	8.30	11.18
SSD [69]	✗	9.58	12.15
TFPOC [75]	✗	10.97	14.24
UPC [76]	✗	7.83	9.74
CountDiff [78]	✗	8.36	10.84
<i>Open-world Text-guided</i>			
CountTX [84]	✗	11.64	14.85
CLIP-Count [85]	✗	11.96	16.61
VLCounter [86]	✗	6.46	8.68
VA-Count [88]	✗	10.63	13.20
TFPOC [‡] [75]	✗	11.01	14.34
UPC [76] [‡]	✗	7.62	9.71
CountDiff [78] [‡]	✗	10.32	12.92

[‡] prompt-based modification of a reference-based method.

errors on some images. The logical conclusion is that, as of today, the core challenge of effective guidance in class-agnostic counting entails a quantifiable cost in accuracy—a trade-off that should be central to both the evaluation and future development of CAC methods.

F. Cross-dataset Generalization

Table III summarizes the results on the CARPK dataset [43] among methods that reported outcomes on this benchmark.

Fine-tuned reference-based approaches demonstrate substantial performance gains compared to non-fine-tuned ones, as expected, since the latter do not see the vehicle category at all. In contrast, experiments on CARPK with fine-tuned models diverge slightly from the CAC paradigm, as the model is tested on the same class seen during fine-tuning. Rather than evaluating generalization to unseen categories, as in the standard CAC setting, this scenario assesses the ability to learn from a small number of exemplars and generalize across a dataset containing objects of the same category. Specifically,

CACViT [73] leads the pack of fine-tuned techniques (MAE: 4.91, RMSE: 6.49). Its performance likely stems from the use of a pre-trained Vision Transformer that performs unified feature extraction and matching via attention mechanisms. The model processes the query image and exemplar patches as token sequences—referred to as query and exemplar tokens—which are concatenated and jointly fed into the transformer encoder. Within this unified token space, self-attention extracts contextual features from both inputs and simultaneously performs similarity matching between them. This design appears particularly effective in learning from very few exemplars (12 in this case), and demonstrates robustness in generalizing across the dataset. BMNet+ [63] and SAFECount [66] also deliver strong results (MAEs of 5.76 and 5.33, respectively), leveraging advanced similarity modules and data-driven refinement strategies that enhance adaptability.

Non-fine-tuned methods generally show higher error rates, yet recent models like LOCA [67], SATCount [70], CACViT [73], and SSD [69] narrow the gap with fine-tuned approaches. This set of experiments fully reflects the CAC setting, since models have not seen the vehicle category during training. The goal here is to evaluate their ability to count a specific object category in a new dataset under domain shift. Notably, UPC [76] achieves the best performance among non-fine-tuned methods (MAE: 7.84, RMSE: 9.74), and remains competitive even in open-world text-guided settings (MAE: 7.62, RMSE: 9.71). UPC’s strong generalization may be attributed to its iterative refinement mechanism, which progressively updates the predicted density map by reusing it as a new prompt. This feedback loop allows the model to converge toward consistent outputs and may help suppress spurious activations in unfamiliar domains. Additionally, the use of a contrastive training strategy—where the model learns to distinguish between prompts that match the target object and those that do not—encourages the network to focus on semantically meaningful regions. These mechanisms likely improve the model’s robustness to domain shift by reinforcing object-specific consistency and reducing reliance on dataset-specific context. Notably, VLCounter [86] stands out among open-world text-guided methods (MAE: 6.46, RMSE: 8.68), but UPC’s performance remains notable given its unified prompt representation and refinement strategy.

G. Textual Semantic Understanding

Recently, [126] highlighted notable weaknesses in state-of-the-art open-world text-guided CAC methods. Specifically, the authors argued that these models often fail to accurately identify *which* object class needs to be counted based on the textual description. Instead, they tend to count instances of the predominant class, disregarding the true intent of the prompt. To address these shortcomings, the authors introduced a novel benchmark, including a test suite specifically designed to evaluate these limitations in current evaluation systems.

Table IV presents results on the FSC-147 dataset, focusing on their negative-label test. This test evaluates the performance of the model on single-class images by prompting it with textual descriptions referencing absent object classes. [126]

TABLE IV

TEXTUAL SEMANTIC UNDERSTANDING RESULTS. WE ILLUSTRATE THE RESULTS ON THE FSC-147 DATASET AS REPORTED IN [126], WHERE THE AUTHORS INTRODUCED A TEST SUITE DESIGNED TO EVALUATE IF OPEN-WORLD TEST-GUIDED CAC METHODS ARE TRULY ABLE TO UNDERSTAND THE PROVIDED TEXTUAL PROMPTS. THE BEST RESULTS ARE IN BOLD.

Method	Validation Set		Test Set	
	NMN ↓	PCCN ↑	NMN ↓	PCCN ↑
CounTX [84]	0.87	69.79	0.95	64.51
CLIP-Count [85]	1.24	48.11	1.27	38.13
VLCounter [86]	1.07	62.70	1.15	53.36
TFPOC [75]	0.67	62.62	0.75	66.04
DAVE [74]	0.13	95.90	0.08	97.62

introduced also two metrics for the assessment of this test: (i) the normalized mean of negative predictions (NMN), which is the absolute counting error computed by prompting the model with the negative classes, normalized by the ground truth of the positive class, and (ii) the positive class count nearness (PCCN) that mixes positive and negative class predictions, providing an overall quantitative assessment of strong failures in the model. More details can be found in [126]. DAVE [74] performs exceptionally well across nearly all metrics proposed in [126], standing out as the best-performing model in this challenging scenario. Although the authors noted that DAVE occasionally produces catastrophic errors due to sporadic outliers, it remains the top performer overall in this evaluation.

H. Computational Complexity

Table V reports the computational complexity—measured in GFLOPs and number of parameters—of the most representative CAC methods, i.e., those highlighted in Fig. 3. Specifically, we include values reported in the original papers when available, and compute them for methods that provide public code but omit complexity metrics. Models lacking both reported values and code are excluded from the analysis.

The results reveal substantial variability in computational requirements across paradigms and architectures. Among reference-based methods, models such as FamNet [32] and BMNet+ [63] are relatively lightweight, requiring 55 and 27 GFLOPs, respectively, with moderate parameter counts (26M and 13M). In contrast, more recent architectures like SAFECount [66] and LOCA [67] show a marked increase in both GFLOPs (366 and 80) and parameters (32M and 37M), reflecting the adoption of deeper backbones and more sophisticated matching modules. DAVE [74] represents a particularly interesting case since it stands out as the state-of-the-art in terms of accuracy, achieving the lowest MAE and RMSE on both FSC-147 [32] and CARPK [43]. However, this performance comes at a very high computational cost: 1515 GFLOPs and 47M parameters—an order of magnitude higher than most other methods. This makes DAVE ideal for high-resource environments, but potentially unsuitable for edge deployment.

In the open-world text-guided paradigm, computational demands are generally higher due to the integration of

TABLE V

COMPUTATIONAL COMPLEXITY ANALYSIS. WE REPORT THE COMPUTATIONAL COMPLEXITY OF THE MOST REPRESENTATIVE CAC METHODS IN TERMS OF GFLOPs AND NUMBER OF PARAMETERS. “-” INDICATES THAT THE VALUES WERE NOT COMPUTED BECAUSE THE AUTHORS DID NOT PROVIDE A PRETRAINED MODEL. THE BEST RESULTS ARE HIGHLIGHTED IN BOLD.

Method	GFLOPs ↓	#Parameters ↓
<i>Reference-based</i>		
FamNet [32]	55	26M
RCAC [‡] [62]	-	10M
BMNet+ [63]	27	13M
SAFECount [66]	366	32M
LOCA [67]	80	37M
SSD [‡] [69]	-	36M
CACViT [73]	89	99M
DAVE [‡] [74]	1,515	47M
TFPOC [‡] [75]	102	94M
CounTR ^{‡§} [81]	84	99M
<i>Open-world Text-guided</i>		
ZSC [‡] [83]	-	12M
CounTX [‡] [84]	50	161M
CLIP-Count [‡] [85]	27	166M
VLCounter [86]	68	1.4M
GroundingREC [‡] [87]	69	173M
VA-Count [‡] [88]	-	99M

[‡] computed in this work; [§] reference-based modification of a reference-less method.

large vision-language models. For instance, CounTX [84] and GroundingREC [87] reach parameter counts of 161M and 173M, respectively. Notably, VLCounter [86] achieves a remarkably low parameter count (1.4M) while maintaining competitive GFLOPs (68), thanks to efficient prompt-tuning and segment-aware skip connections.

Overall, the analysis reveals that higher computational complexity does not always correlate with better performance. While DAVE justifies its cost with top-tier accuracy, other models like CACViT, SSD, and BMNet+ offer a more favorable trade-off between efficiency and accuracy. These findings suggest that architectural innovations—rather than brute-force scaling—are key to achieving practical and scalable CAC solutions.

I. Qualitative Comparison

Fig. 6 presents qualitative results for reference-based CAC techniques. We compare the outputs of the most representative CAC models (see Fig. 3) for which pretrained weights are publicly available. Specifically, we show both easy and hard samples, with the latter often corresponding to failure cases. Note that, for TFPOC [75], density maps were generated from the predicted masks by placing a small circle at the centroid of each mask.

Overall, DAVE [74] confirms its state-of-the-art performance. However, it is worth noting that even DAVE, like all other models, struggles with certain challenging samples. One recurring challenge appears to be related to object density—objects tend to overlap in crowded scenes. This issue becomes more pronounced when additional elements such as background clutter and distractors are present, as in the second

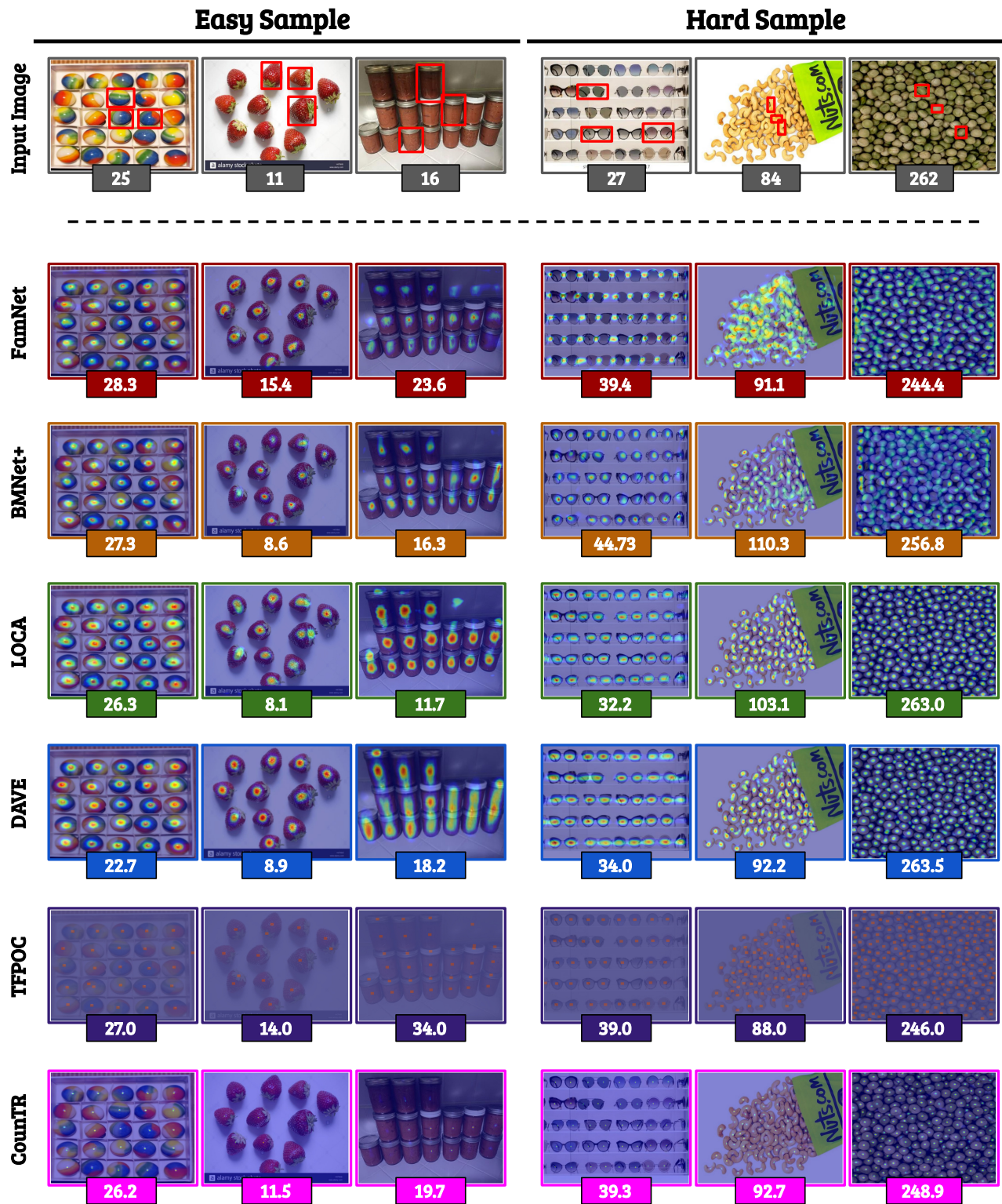


Fig. 6. **Qualitative results of reference-based CAC methods.** We report some qualitative results of the most representative reference-based CAC techniques. On the left, we show three easy samples, while on the right, three challenging samples that result in large counting errors.

hard sample. In contrast, it is less evident in scenarios where only the target objects are present and are relatively uniformly distributed, as in the third hard sample. A particularly interesting failure case is illustrated by the first hard sample. Despite the absence of occlusion and the seemingly simple scene, all

models consistently fail by counting the lenses of the glasses rather than the glasses as whole objects. This suggests that the models are unable to build effective representations of the exemplars and instead rely on detecting repetitive patterns in the image.

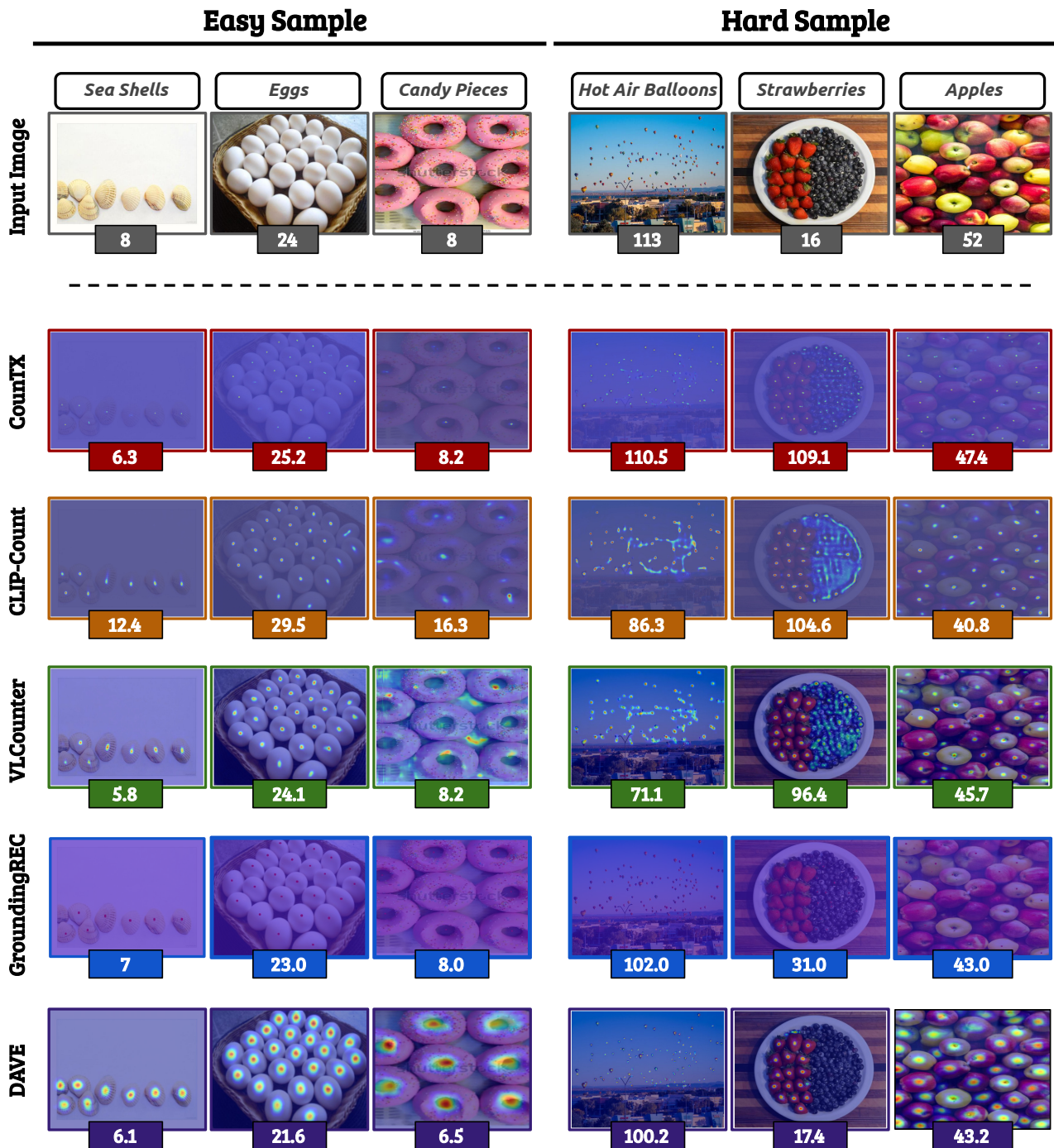


Fig. 7. **Qualitative results of open-world text-guided CAC methods.** We report some qualitative results of the most representative open-world text-guided CAC techniques. On the left are three easy samples, while on the right are three challenging samples that result in large counting errors.

Fig. 7 presents instead qualitative results for the most representative open-world text-guided CAC methods. Note that, for GroundingREC [87], density maps were generated by placing a small circle at the centroids of the generated bounding boxes. The most pronounced and interesting failure case is observed in the second hard sample. As previously noted by [126] and discussed in Sec. V-G, this error stems from the limited ability of the models to understand the semantic content of textual descriptions. In particular, they tend to count repeated objects regardless of the actual meaning conveyed by the text.

This issue is clearly illustrated in the image, which contains a large number of objects from two distinct categories. Only DAVE [74], and to a lesser extent GroundingREC [87], can successfully address this challenge.

VI. CONCLUSION AND OPEN CHALLENGES

Class-agnostic counting has become a pivotal field in object counting, addressing the limitations of traditional class-specific methods. Unlike conventional approaches that require extensive labeled data for each object category, CAC enables models

to count objects across arbitrary categories, including those unseen during training. For the first time, this survey reviewed the evolution of CAC methodologies, categorizing them into three paradigms: reference-based, reference-less, and open-world text-guided approaches. Each paradigm brings distinct advantages and trade-offs, reflecting the diverse demands of real-world applications. Reference-based methods, which rely on annotated exemplars, set the benchmark for accuracy and robustness. However, their dependence on labeled exemplars limits scalability and automation. Reference-less approaches address this by automatically identifying dominant object classes, offering greater flexibility but still lagging behind in performance. Open-world text-guided methods further increase adaptability by allowing object specification via textual prompts, yet—like reference-less methods—this flexibility comes at the cost of reduced accuracy compared to exemplar-based approaches.

Through an in-depth analysis of state-of-the-art methods on benchmarks such as FSC-147 [32] and CARPK [43], this survey highlights both notable advancements and persistent challenges. While DAVE [74] leads the reference-based paradigm on FSC-147 (MAE: 8.66, RMSE: 32.36), the reference-less and text-guided leaderboards remain less conclusive. CounTR [81] and GCNet [82] stand out among reference-less methods, the latter notable for its weak supervision. In the text-guided setting, GroundingREC [87] achieves the lowest MAE, while DAVE remains robust to outliers. Cross-dataset evaluations on CARPK reveal that CACViT [73], UPC [76], and VLCounter [86] generalize best across paradigms. Qualitative results further confirm that even top-performing models can fail in cluttered or ambiguous scenes, often due to poor or missing guidance. Moreover, recent benchmarks [126] show that open-world models frequently misinterpret prompts, highlighting limitations in semantic understanding.

Open challenges span all paradigms. A major limitation is the lack of diverse and publicly available datasets. The gold standard, FSC-147, has several drawbacks. First, it contains a limited number of images and object classes. Furthermore, as pointed out in [126], almost all images contain only a single class of objects. Multi-class images would be a desirable feature for new datasets, as objects belonging to classes different from the one being counted could act as distractors for the counting approach. The lack of diverse and large-scale datasets also leads to challenges in designing learning approaches suited for data-scarce scenarios. Among the analyzed methods, only RCC [80] and GCNet [82] operate with weak supervision, avoiding the use of dot annotations. This setting is particularly promising, as it could help mitigate the challenge of creating large-scale labeled datasets for the counting task. Recently, an emerging direction is to incorporate completely unsupervised components into CAC pipelines [127], [128], although current performance remains far from state-of-the-art.

Other challenges are more specific to open-world text-guided methodologies, which appear to represent the future. These models have been shown to occasionally misinterpret the meaning of prompts. Although some architectures demonstrate relative robustness, further improvements are needed. New architectural designs and learning strategies—such as

contrastive learning over classes not present in the images—should be explored. Another particularly interesting direction concerns the use of richer textual inputs to enable context-aware prompting. Future research could investigate automatic prompt generation techniques to produce more informative and targeted textual queries. While current large multimodal models are not yet effective for counting tasks, partly due to limitations in visual token capacity, their contextual priors and exposure to diverse visual-textual data suggest potential for future exploration, especially as architectures evolve to better handle fine-grained visual details. Beyond these technical challenges, our analysis underscores a broader issue: the convenience offered by reference-less and text-guided paradigms comes at a measurable cost in accuracy. Bridging this gap—by developing methods that match the guidance quality of human-provided exemplars without manual intervention—remains a key open challenge. Finally, our computational complexity analysis reveals that top-performing models such as DAVE achieve state-of-the-art accuracy at the cost of significantly higher GFLOPs and parameter counts. This highlights a critical trade-off between performance and efficiency, which must be carefully considered when designing CAC systems for real-world deployment, particularly in resource-constrained environments.

REFERENCES

- [1] V. S. Lempitsky and A. Zisserman, "Learning to count objects in images," in *Advances in Neural Information Processing Systems 23: 24th Annual Conference on Neural Information Processing Systems 2010. Proceedings of a meeting held 6-9 December 2010, Vancouver, British Columbia, Canada*. Curran Associates, Inc., 2010, pp. 1324–1332.
- [2] D. B. Sam, S. Surya, and R. V. Babu, "Switching convolutional neural network for crowd counting," in *2017 IEEE Conference on Computer Vision and Pattern Recognition, CVPR 2017, Honolulu, HI, USA, July 21-26, 2017*. IEEE Computer Society, 2017, pp. 4031–4039.
- [3] L. Boominathan, S. S. S. Kruthiventi, and R. V. Babu, "Crowdnet: A deep convolutional network for dense crowd counting," in *Proceedings of the 2016 ACM Conference on Multimedia Conference, MM 2016, Amsterdam, The Netherlands, October 15-19, 2016*. ACM, 2016, pp. 640–644.
- [4] C. Zhang, H. Li, X. Wang, and X. Yang, "Cross-scene crowd counting via deep convolutional neural networks," in *IEEE Conference on Computer Vision and Pattern Recognition, CVPR 2015, Boston, MA, USA, June 7-12, 2015*. IEEE Computer Society, 2015, pp. 833–841.
- [5] Z. Shi, L. Zhang, Y. Liu, X. Cao, Y. Ye, M. Cheng, and G. Zheng, "Crowd counting with deep negative correlation learning," in *2018 IEEE Conference on Computer Vision and Pattern Recognition, CVPR 2018, Salt Lake City, UT, USA, June 18-22, 2018*. Computer Vision Foundation / IEEE Computer Society, 2018, pp. 5382–5390.
- [6] W. Liu, M. Salzmann, and P. Fua, "Context-aware crowd counting," in *IEEE Conference on Computer Vision and Pattern Recognition, CVPR 2019, Long Beach, CA, USA, June 16-20, 2019*. Computer Vision Foundation / IEEE, 2019, pp. 5099–5108.
- [7] M. A. Hossain, M. Hosseinzadeh, O. Chanda, and Y. Wang, "Crowd counting using scale-aware attention networks," in *IEEE Winter Conference on Applications of Computer Vision, WACV 2019, Waikoloa Village, HI, USA, January 7-11, 2019*. IEEE, 2019, pp. 1280–1288.
- [8] X. Cao, Z. Wang, Y. Zhao, and F. Su, "Scale aggregation network for accurate and efficient crowd counting," in *Computer Vision - ECCV 2018 - 15th European Conference, Munich, Germany, September 8-14, 2018, Proceedings, Part V*, ser. Lecture Notes in Computer Science, vol. 11209. Springer, 2018, pp. 757–773.
- [9] M. Avvenuti, M. Bongiovanni, L. Ciampi, F. Falchi, C. Gennaro, and N. Messina, "A spatio-temporal attentive network for video-based crowd counting," in *IEEE Symposium on Computers and Communications, ISCC 2022, Rhodes, Greece, June 30 - July 3, 2022*. IEEE, 2022, pp. 1–6.

- [10] M. D. Benedetto, F. Carrara, L. Ciampi, F. Falchi, C. Gennaro, and G. Amato, "An embedded toolset for human activity monitoring in critical environments," *Expert Syst. Appl.*, vol. 199, p. 117125, 2022.
- [11] Z. Zhao and X. Li, "Deformable density estimation via adaptive representation," *IEEE Trans. Image Process.*, vol. 32, pp. 1134–1144, 2023.
- [12] E. C. Del Re, *Collective Behavior*. Dordrecht: Springer Netherlands, 2013, pp. 422–429.
- [13] A. F. Aveni, "The not-so-lonely crowd: Friendship groups in collective behavior," *Sociometry*, vol. 40, no. 1, pp. 96–99, 1977.
- [14] M. Biggs, "Size matters: Quantifying protest by counting participants," *Sociological Methods & Research*, vol. 47, no. 3, pp. 351–383, 2018.
- [15] A. F. Abdelghany, K. F. Abdelghany, H. S. Mahmassani, and W. Alhalabi, "Modeling framework for optimal evacuation of large-scale crowded pedestrian facilities," *Eur. J. Oper. Res.*, vol. 237, no. 3, pp. 1105–1118, 2014.
- [16] M. Tian, H. Guo, H. Chen, Q. Wang, C. Long, and Y. Ma, "Automated pig counting using deep learning," *Comput. Electron. Agric.*, vol. 163, 2019.
- [17] F. Sarwar, A. Griffin, P. Periasamy, K. Portas, and J. Law, "Detecting and counting sheep with a convolutional neural network," in *15th IEEE International Conference on Advanced Video and Signal Based Surveillance, AVSS 2018, Auckland, New Zealand, November 27-30, 2018*. IEEE, 2018, pp. 1–6.
- [18] L. Ciampi, V. Zeni, L. Incrocci, A. Canale, G. Benelli, F. Falchi, G. Amato, and S. Chessa, "A deep learning-based pipeline for whitefly pest abundance estimation on chromotropic sticky traps," *Ecol. Informatics*, vol. 78, p. 102384, 2023.
- [19] T. Alkhudaydi, J. Zhou, and B. de la Iglesia, "Spikeletfcn: Counting spikelets from infield wheat crop images using fully convolutional networks," in *Artificial Intelligence and Soft Computing - 18th International Conference, ICAISC 2019, Zakopane, Poland, June 16-20, 2019, Proceedings, Part I*, ser. Lecture Notes in Computer Science, vol. 11508. Springer, 2019, pp. 3–13.
- [20] H. Lu, Z. Cao, Y. Xiao, B. Zhuang, and C. Shen, "Tasselnet: Counting maize tassels in the wild via local counts regression network," *CoRR*, vol. abs/1707.02290, 2017.
- [21] M. P. Pound, J. A. Atkinson, D. M. Wells, T. P. Pridmore, and A. P. French, "Deep learning for multi-task plant phenotyping," in *2017 IEEE International Conference on Computer Vision Workshops, ICCV Workshops 2017, Venice, Italy, October 22-29, 2017*. IEEE Computer Society, 2017, pp. 2055–2063.
- [22] Z. Dai, H. Song, X. Wang, Y. Fang, X. Yun, Z. Zhang, and H. Li, "Video-based vehicle counting framework," *IEEE Access*, vol. 7, pp. 64460–64470, 2019.
- [23] H. Tayara, K. G. Soo, and K. T. Chong, "Vehicle detection and counting in high-resolution aerial images using convolutional regression neural network," *IEEE Access*, vol. 6, pp. 2220–2230, 2018.
- [24] S. Zhang, G. Wu, J. P. Costeira, and J. M. F. Moura, "Fcn-rlstm: Deep spatio-temporal neural networks for vehicle counting in city cameras," in *IEEE International Conference on Computer Vision, ICCV 2017, Venice, Italy, October 22-29, 2017*. IEEE Computer Society, 2017, pp. 3687–3696.
- [25] G. Amato, L. Ciampi, F. Falchi, and C. Gennaro, "Counting vehicles with deep learning in onboard UAV imagery," in *2019 IEEE Symposium on Computers and Communications, ISCC 2019, Barcelona, Spain, June 29 - July 3, 2019*. IEEE, 2019, pp. 1–6.
- [26] L. Ciampi, C. Gennaro, F. Carrara, F. Falchi, C. Vairo, and G. Amato, "Multi-camera vehicle counting using edge-ai," *Expert Syst. Appl.*, vol. 207, p. 117929, 2022.
- [27] V. Balaska, D. Folinias, F. K. Konstantinidis, and A. Gasteratos, "Smart counting of unboxed stocks in the warehouse 4.0 ecosystem," in *IEEE International Conference on Imaging Systems and Techniques, IST 2022, Kaohsiung, Taiwan, June 21-23, 2022*. IEEE, 2022, pp. 1–6.
- [28] J. P. Cohen, G. Boucher, C. A. Glastonbury, H. Z. Lo, and Y. Bengio, "Count-ception: Counting by fully convolutional redundant counting," in *2017 IEEE International Conference on Computer Vision Workshops, ICCV Workshops 2017, Venice, Italy, October 22-29, 2017*. IEEE Computer Society, 2017, pp. 18–26.
- [29] L. Ciampi, F. Carrara, V. Totaro, R. Mazziotti, L. Lupori, C. Santiago, G. Amato, T. Pizzorusso, and C. Gennaro, "Learning to count biological structures with raters' uncertainty," *Medical Image Anal.*, vol. 80, p. 102500, 2022.
- [30] R. Zhu, D. Sui, H. Qin, and A. Hao, "An extended type cell detection and counting method based on FCN," in *17th IEEE International Conference on Bioinformatics and Bioengineering, BIBE 2017, Washington, DC, USA, October 23-25, 2017*. IEEE Computer Society, 2017, pp. 51–56.
- [31] W. Xie, J. A. Noble, and A. Zisserman, "Microscopy cell counting and detection with fully convolutional regression networks," *Comput. methods Biomech. Biomed. Eng. Imaging Vis.*, vol. 6, no. 3, pp. 283–292, 2018.
- [32] V. Ranjan, U. Sharma, T. Nguyen, and M. Hoai, "Learning to count everything," in *IEEE Conference on Computer Vision and Pattern Recognition, CVPR 2021, virtual, June 19-25, 2021*. Computer Vision Foundation / IEEE, 2021, pp. 3394–3403.
- [33] H. Liu, C. Li, Q. Wu, and Y. J. Lee, "Visual instruction tuning," in *Advances in Neural Information Processing Systems 36: Annual Conference on Neural Information Processing Systems 2023, NeurIPS 2023, New Orleans, LA, USA, December 10 - 16, 2023*, 2023.
- [34] D. Zhu, J. Chen, X. Shen, X. Li, and M. Elhoseiny, "Minigt-4: Enhancing vision-language understanding with advanced large language models," *CoRR*, vol. abs/2304.10592, 2023.
- [35] Q. Ye, H. Xu, G. Xu, J. Ye, M. Yan, Y. Zhou, J. Wang, A. Hu, P. Shi, Y. Shi, C. Li, Y. Xu, H. Chen, J. Tian, Q. Qi, J. Zhang, and F. Huang, "mplug-owl: Modularization empowers large language models with multimodality," *CoRR*, vol. abs/2304.14178, 2023.
- [36] Z. Yin, J. Wang, J. Cao, Z. Shi, D. Liu, M. Li, X. Huang, Z. Wang, L. Sheng, L. Bai, J. Shao, and W. Ouyang, "LAMM: language-assisted multi-modal instruction-tuning dataset, framework, and benchmark," in *Advances in Neural Information Processing Systems 36: Annual Conference on Neural Information Processing Systems 2023, NeurIPS 2023, New Orleans, LA, USA, December 10 - 16, 2023*, 2023.
- [37] E. Lu, W. Xie, and A. Zisserman, "Class-agnostic counting," in *Computer Vision - ACCV 2018 - 14th Asian Conference on Computer Vision, Perth, Australia, December 2-6, 2018, Revised Selected Papers, Part III*, ser. Lecture Notes in Computer Science, vol. 11363. Springer, 2018, pp. 669–684.
- [38] C. Finn, P. Abbeel, and S. Levine, "Model-agnostic meta-learning for fast adaptation of deep networks," in *Proceedings of the 34th International Conference on Machine Learning, ICML 2017, Sydney, NSW, Australia, 6-11 August 2017*, ser. Proceedings of Machine Learning Research, vol. 70. PMLR, 2017, pp. 1126–1135.
- [39] O. Vinyals, C. Blundell, T. Lillicrap, K. Kavukcuoglu, and D. Wierstra, "Matching networks for one shot learning," in *Advances in Neural Information Processing Systems 29: Annual Conference on Neural Information Processing Systems 2016, December 5-10, 2016, Barcelona, Spain*, 2016, pp. 3630–3638.
- [40] Q. Wang, J. Gao, W. Lin, and Y. Yuan, "Learning from synthetic data for crowd counting in the wild," in *IEEE Conference on Computer Vision and Pattern Recognition, CVPR 2019, Long Beach, CA, USA, June 16-20, 2019*. Computer Vision Foundation / IEEE, 2019, pp. 8198–8207.
- [41] L. Ciampi, C. Santiago, J. P. Costeira, C. Gennaro, and G. Amato, "Domain adaptation for traffic density estimation," in *Proceedings of the 16th International Joint Conference on Computer Vision, Imaging and Computer Graphics Theory and Applications, VISIGRAPP 2021, Volume 5: VISAPP, Online Streaming, February 8-10, 2021*. SCITEPRESS, 2021, pp. 185–195.
- [42] M. Oh, P. A. Olsen, and K. N. Ramamurthy, "Crowd counting with decomposed uncertainty," in *The Thirty-Fourth AAAI Conference on Artificial Intelligence, AAAI 2020, The Thirty-Second Innovative Applications of Artificial Intelligence Conference, IAAI 2020, The Tenth AAAI Symposium on Educational Advances in Artificial Intelligence, EAAI 2020, New York, NY, USA, February 7-12, 2020*. AAAI Press, 2020, pp. 11799–11806.
- [43] M. Hsieh, Y. Lin, and W. H. Hsu, "Drone-based object counting by spatially regularized regional proposal network," in *IEEE International Conference on Computer Vision, ICCV 2017, Venice, Italy, October 22-29, 2017*. IEEE Computer Society, 2017, pp. 4165–4173.
- [44] V. A. Sindagi and V. M. Patel, "A survey of recent advances in cnn-based single image crowd counting and density estimation," *Pattern Recognit. Lett.*, vol. 107, pp. 3–16, 2018.
- [45] B. Li, H. Huang, A. Zhang, P. Liu, and C. Liu, "Approaches on crowd counting and density estimation: a review," *Pattern Anal. Appl.*, vol. 24, no. 3, pp. 853–874, 2021.
- [46] G. Gao, J. Gao, Q. Liu, Q. Wang, and Y. Wang, "Cnn-based density estimation and crowd counting: A survey," *CoRR*, vol. abs/2003.12783, 2020.
- [47] R. Gouiaa, M. A. Akhloufi, and M. Shahbazi, "Advances in convolution neural networks based crowd counting and density estimation," *Big Data Cogn. Comput.*, vol. 5, no. 4, p. 50, 2021.

- [48] A. Patwal, M. Diwakar, V. Tripathi, and P. Singh, "Crowd counting analysis using deep learning: a critical review," *Procedia Computer Science*, vol. 218, pp. 2448–2458, 2023, international Conference on Machine Learning and Data Engineering.
- [49] H. Bai, J. Mao, and S. G. Chan, "A survey on deep learning-based single image crowd counting: Network design, loss function and supervisory signal," *Neurocomputing*, vol. 508, pp. 1–18, 2022.
- [50] M. A. Khan, H. Menouar, and R. Hamila, "Revisiting crowd counting: State-of-the-art, trends, and future perspectives," *Image Vis. Comput.*, vol. 129, p. 104597, 2023.
- [51] W. Jingying, "A survey on crowd counting methods and datasets," in *Advances in Computer, Communication and Computational Sciences*. Singapore: Springer Singapore, 2021, pp. 851–863.
- [52] K. B. A. Hassen, J. J. M. Machado, and J. M. R. S. Tavares, "Convolutional neural networks and heuristic methods for crowd counting: A systematic review," *Sensors*, vol. 22, no. 14, p. 5286, 2022.
- [53] G. Yang and D. Zhu, "Survey on algorithms of people counting in dense crowd and crowd density estimation," *Multim. Tools Appl.*, vol. 82, no. 9, pp. 13 637–13 648, 2023.
- [54] Y. Hao, H. Du, M. Mao, Y. Liu, and J. Fan, "A survey on regression-based crowd counting techniques," *Inf. Technol. Control.*, vol. 52, no. 3, pp. 693–712, 2023.
- [55] Z. Fan, H. Zhang, Z. Zhang, G. Lu, Y. Zhang, and Y. Wang, "A survey of crowd counting and density estimation based on convolutional neural network," *Neurocomputing*, vol. 472, pp. 224–251, 2022.
- [56] A. D'Alessandro, A. Mahdavi-Amiri, and G. Hamarneh, "Counting objects in images using DeepLearning: Methods and current challenges," jun 2023.
- [57] C. Arteta, V. S. Lempitsky, and A. Zisserman, "Counting in the wild," in *Computer Vision - ECCV 2016 - 14th European Conference, Amsterdam, The Netherlands, October 11-14, 2016, Proceedings, Part VII*, ser. Lecture Notes in Computer Science, vol. 9911. Springer, 2016, pp. 483–498.
- [58] C. Padubidri, A. Kamilaris, S. Karatsiolis, and J. Kamminga, "Counting sea lions and elephants from aerial photography using deep learning with density maps," *Animal Biotelemetry*, vol. 9, no. 1, 2021.
- [59] Y. Zhang, D. Zhou, S. Chen, S. Gao, and Y. Ma, "Single-image crowd counting via multi-column convolutional neural network," in *2016 IEEE Conference on Computer Vision and Pattern Recognition, CVPR 2016, Las Vegas, NV, USA, June 27-30, 2016*. IEEE Computer Society, 2016, pp. 589–597.
- [60] S. Yang, H. Su, W. H. Hsu, and W. Chen, "Class-agnostic few-shot object counting," in *IEEE Winter Conference on Applications of Computer Vision, WACV 2021, Waikoloa, HI, USA, January 3-8, 2021*. IEEE, 2021, pp. 869–877.
- [61] V. Ranjan and M. Hoai, "Vicinal counting networks," in *IEEE/CVF Conference on Computer Vision and Pattern Recognition Workshops, CVPR Workshops 2022, New Orleans, LA, USA, June 19-20, 2022*. IEEE, 2022, pp. 4220–4229.
- [62] S. Gong, S. Zhang, J. Yang, D. Dai, and B. Schiele, "Class-agnostic object counting robust to intraclass diversity," in *Computer Vision - ECCV 2022 - 17th European Conference, Tel Aviv, Israel, October 23-27, 2022, Proceedings, Part XXXIII*, ser. Lecture Notes in Computer Science, vol. 13693. Springer, 2022, pp. 388–403.
- [63] M. Shi, H. Lu, C. Feng, C. Liu, and Z. Cao, "Represent, compare, and learn: A similarity-aware framework for class-agnostic counting," in *IEEE/CVF Conference on Computer Vision and Pattern Recognition, CVPR 2022, New Orleans, LA, USA, June 18-24, 2022*. IEEE, 2022, pp. 9519–9528.
- [64] W. Lin, K. Yang, X. Ma, J. Gao, L. Liu, S. Liu, J. Hou, S. Yi, and A. B. Chan, "Scale-prior deformable convolution for exemplar-guided class-agnostic counting," in *33rd British Machine Vision Conference 2022, BMVC 2022, London, UK, November 21-24, 2022*. BMVA Press, 2022, p. 313.
- [65] T. McCarthy, J. J. Virtusio, J. J. M. Ople, D. S. Tan, D. Amalin, and K. Hua, "MACnet: Mask augmented counting network for class-agnostic counting," *Pattern Recognit. Lett.*, vol. 169, pp. 75–80, 2023.
- [66] Z. You, K. Yang, W. Luo, X. Lu, L. Cui, and X. Le, "Few-shot object counting with similarity-aware feature enhancement," in *IEEE/CVF Winter Conference on Applications of Computer Vision, WACV 2023, Waikoloa, HI, USA, January 2-7, 2023*. IEEE, 2023, pp. 6304–6313.
- [67] N. Đukic, A. Lukezic, V. Zavrtnik, and M. Kristan, "A low-shot object counting network with iterative prototype adaptation," in *IEEE/CVF International Conference on Computer Vision, ICCV 2023, Paris, France, October 1-6, 2023*. IEEE, 2023, pp. 18 826–18 835.
- [68] A. F. O. Soliven, J. J. Virtusio, J. J. M. Ople, D. S. Tan, D. Amalin, and K. Hua, "Conconet: Class-agnostic counting with positive and negative exemplars," *Pattern Recognit. Lett.*, vol. 171, pp. 148–154, 2023.
- [69] Y. Xu, F. Song, and H. Zhang, "Learning spatial similarity distribution for few-shot object counting," in *Proceedings of the Thirty-Third International Joint Conference on Artificial Intelligence, IJCAI 2024, Jeju, South Korea, August 3-9, 2024*. ijcai.org, 2024, pp. 1507–1515.
- [70] Y. Wang, B. Yang, X. Wang, C. Liang, and J. Chen, "Satcount: A scale-aware transformer-based class-agnostic counting framework," *Neural Networks*, vol. 172, p. 106126, 2024.
- [71] B. Gao and Z. Huang, "Cstrans: Correlation-guided self-activation transformer for counting everything," *Pattern Recognit.*, vol. 153, p. 110556, 2024.
- [72] H. Yang, S. Cai, B. Deng, M. Wei, and Y. Zhang, "Versatile correlation learning for size-robust generalized counting: A new perspective," *Knowl. Based Syst.*, vol. 286, p. 111394, 2024.
- [73] Z. Wang, L. Xiao, Z. Cao, and H. Lu, "Vision transformer off-the-shelf: A surprising baseline for few-shot class-agnostic counting," in *Thirty-Eighth AAAI Conference on Artificial Intelligence, AAAI 2024, Thirty-Sixth Conference on Innovative Applications of Artificial Intelligence, IAAI 2024, Fourteenth Symposium on Educational Advances in Artificial Intelligence, EAAI 2014, February 20-27, 2024, Vancouver, Canada*. AAAI Press, 2024, pp. 5832–5840.
- [74] J. Pelhan, A. Lukezic, V. Zavrtnik, and M. Kristan, "DAVE - A detect-and-verify paradigm for low-shot counting," in *IEEE/CVF Conference on Computer Vision and Pattern Recognition, CVPR 2024, Seattle, WA, USA, June 16-22, 2024*. IEEE, 2024, pp. 23 293–23 302.
- [75] Z. Shi, Y. Sun, and M. Zhang, "Training-free object counting with prompts," in *IEEE/CVF Winter Conference on Applications of Computer Vision, WACV 2024, Waikoloa, HI, USA, January 3-8, 2024*. IEEE, 2024, pp. 322–330.
- [76] W. Lin and A. B. Chan, "A fixed-point approach to unified prompt-based counting," in *Thirty-Eighth AAAI Conference on Artificial Intelligence, AAAI 2024, Thirty-Sixth Conference on Innovative Applications of Artificial Intelligence, IAAI 2024, Fourteenth Symposium on Educational Advances in Artificial Intelligence, EAAI 2014, February 20-27, 2024, Vancouver, Canada*. AAAI Press, 2024, pp. 3468–3476.
- [77] Z. Huang, M. Dai, Y. Zhang, J. Zhang, and H. Shan, "Point, segment and count: A generalized framework for object counting," in *IEEE/CVF Conference on Computer Vision and Pattern Recognition, CVPR 2024, Seattle, WA, USA, June 16-22, 2024*. IEEE, 2024, pp. 17 067–17 076.
- [78] X. Hui, Q. Wu, H. Rahmani, and J. Liu, "Class-agnostic object counting with text-to-image diffusion model," in *Computer Vision - ECCV 2024 - 18th European Conference, Milan, Italy, September 29-October 4, 2024, Proceedings, Part LXIX*, ser. Lecture Notes in Computer Science, vol. 15127. Springer, 2024, pp. 1–18.
- [79] V. Ranjan and M. H. Nguyen, "Exemplar free class agnostic counting," in *Computer Vision - ACCV 2022 - 16th Asian Conference on Computer Vision, Macao, China, December 4-8, 2022, Proceedings, Part IV*, ser. Lecture Notes in Computer Science, vol. 13844. Springer, 2022, pp. 71–87.
- [80] M. A. Hobley and V. Prisacariu, "Learning to count anything: Reference-less class-agnostic counting with weak supervision," *CoRR*, vol. abs/2205.10203, 2022.
- [81] C. Liu, Y. Zhong, A. Zisserman, and W. Xie, "Countr: Transformer-based generalised visual counting," in *33rd British Machine Vision Conference 2022, BMVC 2022, London, UK, November 21-24, 2022*. BMVA Press, 2022, p. 370.
- [82] M. Wang, Y. Li, J. Zhou, G. W. Taylor, and M. Gong, "Gcnet: Probing self-similarity learning for generalized counting network," *Pattern Recognit.*, vol. 153, p. 110513, 2024.
- [83] J. Xu, H. Le, V. Nguyen, V. Ranjan, and D. Samaras, "Zero-shot object counting," in *IEEE/CVF Conference on Computer Vision and Pattern Recognition, CVPR 2023, Vancouver, BC, Canada, June 17-24, 2023*. IEEE, 2023, pp. 15 548–15 557.
- [84] N. Amini-Naieni, K. Amini-Naieni, T. Han, and A. Zisserman, "Open-world text-specified object counting," in *British Machine Vision Conference*, 2023.
- [85] R. Jiang, L. Liu, and C. Chen, "Clip-count: Towards text-guided zero-shot object counting," in *Proceedings of the 31st ACM International Conference on Multimedia, MM 2023, Ottawa, ON, Canada, 29 October 2023- 3 November 2023*. ACM, 2023, pp. 4535–4545.
- [86] S. Kang, W. Moon, E. Kim, and J. Heo, "Vlcounter: Text-aware visual representation for zero-shot object counting," in *Thirty-Eighth AAAI Conference on Artificial Intelligence, AAAI 2024, Thirty-Sixth Conference on Innovative Applications of Artificial Intelligence, IAAI 2024, Fourteenth Symposium on Educational Advances in Artificial*

- Intelligence, EAAI 2014, February 20-27, 2024, Vancouver, Canada.* AAAI Press, 2024, pp. 2714–2722.
- [87] S. Dai, J. Liu, and N. Cheung, “Referring expression counting,” in *IEEE/CVF Conference on Computer Vision and Pattern Recognition, CVPR 2024, Seattle, WA, USA, June 16-22, 2024*. IEEE, 2024, pp. 16 985–16 995.
- [88] H. Zhu, J. Yuan, Z. Yang, Y. Guo, Z. Wang, X. Zhong, and S. He, “Zero-shot object counting with good exemplars,” in *Computer Vision - ECCV 2024 - 18th European Conference, Milan, Italy, September 29-October 4, 2024, Proceedings, Part V*, ser. Lecture Notes in Computer Science, vol. 15063. Springer, 2024, pp. 368–385.
- [89] K. He, X. Zhang, S. Ren, and J. Sun, “Deep residual learning for image recognition,” in *2016 IEEE Conference on Computer Vision and Pattern Recognition, CVPR 2016, Las Vegas, NV, USA, June 27-30, 2016*. IEEE Computer Society, 2016, pp. 770–778.
- [90] R. B. Girshick, “Fast R-CNN,” in *2015 IEEE International Conference on Computer Vision, ICCV 2015, Santiago, Chile, December 7-13, 2015*. IEEE Computer Society, 2015, pp. 1440–1448.
- [91] J. F. Henriques, R. Caseiro, P. Martins, and J. Batista, “High-speed tracking with kernelized correlation filters,” *IEEE Trans. Pattern Anal. Mach. Intell.*, vol. 37, no. 3, pp. 583–596, 2015.
- [92] Z. Xu, S. Zhu, P. Sun, and W. Guo, “Spatio-temporal discriminative correlation filter based object tracking,” in *2019 Chinese Control And Decision Conference (CCDC)*, 2019, pp. 5284–5288.
- [93] Q. Wang, L. Zhang, L. Bertinetto, W. Hu, and P. H. S. Torr, “Fast online object tracking and segmentation: A unifying approach,” in *IEEE Conference on Computer Vision and Pattern Recognition, CVPR 2019, Long Beach, CA, USA, June 16-20, 2019*. Computer Vision Foundation / IEEE, 2019, pp. 1328–1338.
- [94] H. Zhang, I. J. Goodfellow, D. N. Metaxas, and A. Odena, “Self-attention generative adversarial networks,” in *Proceedings of the 36th International Conference on Machine Learning, ICML 2019, 9-15 June 2019, Long Beach, California, USA*, ser. Proceedings of Machine Learning Research, vol. 97. PMLR, 2019, pp. 7354–7363.
- [95] Z. Wang, A. C. Bovik, H. R. Sheikh, and E. P. Simoncelli, “Image quality assessment: from error visibility to structural similarity,” *IEEE Trans. Image Process.*, vol. 13, no. 4, pp. 600–612, 2004.
- [96] Z. Chen, S. Zhang, X. Zheng, X. Zhao, and Y. Kong, “Crowd counting based on multiscale spatial guided perception aggregation network,” *IEEE Trans. Neural Networks Learn. Syst.*, vol. 35, no. 12, pp. 17 465–17 478, 2024.
- [97] I. Goodfellow, J. Pouget-Abadie, M. Mirza, B. Xu, D. Warde-Farley, S. Ozair, A. Courville, and Y. Bengio, “Generative adversarial nets,” in *Advances in Neural Information Processing Systems*, vol. 27. Curran Associates, Inc., 2014.
- [98] K. Musgrave, S. J. Belongie, and S. Lim, “A metric learning reality check,” in *Computer Vision - ECCV 2020 - 16th European Conference, Glasgow, UK, August 23-28, 2020, Proceedings, Part XXV*, ser. Lecture Notes in Computer Science, vol. 12370. Springer, 2020, pp. 681–699.
- [99] J. Dai, H. Qi, Y. Xiong, Y. Li, G. Zhang, H. Hu, and Y. Wei, “Deformable convolutional networks,” in *IEEE International Conference on Computer Vision, ICCV 2017, Venice, Italy, October 22-29, 2017*. IEEE Computer Society, 2017, pp. 764–773.
- [100] X. Zhu, H. Hu, S. Lin, and J. Dai, “Deformable convnets V2: more deformable, better results,” in *IEEE Conference on Computer Vision and Pattern Recognition, CVPR 2019, Long Beach, CA, USA, June 16-20, 2019*. Computer Vision Foundation / IEEE, 2019, pp. 9308–9316.
- [101] Q. Wang, W. Lin, J. Gao, and X. Li, “Density-aware curriculum learning for crowd counting,” *IEEE Trans. Cybern.*, vol. 52, no. 6, pp. 4675–4687, 2022.
- [102] W. Shi, J. Caballero, F. Huszar, J. Totz, A. P. Aitken, R. Bishop, D. Rueckert, and Z. Wang, “Real-time single image and video super-resolution using an efficient sub-pixel convolutional neural network,” in *2016 IEEE Conference on Computer Vision and Pattern Recognition, CVPR 2016, Las Vegas, NV, USA, June 27-30, 2016*. IEEE Computer Society, 2016, pp. 1874–1883.
- [103] O. Russakovsky, J. Deng, H. Su, J. Krause, S. Satheesh, S. Ma, Z. Huang, A. Karpathy, A. Khosla, M. S. Bernstein, A. C. Berg, and L. Fei-Fei, “Imagenet large scale visual recognition challenge,” *Int. J. Comput. Vis.*, vol. 115, no. 3, pp. 211–252, 2015.
- [104] K. Maninis, S. Caelles, J. Pont-Tuset, and L. V. Gool, “Deep extreme cut: From extreme points to object segmentation,” in *2018 IEEE Conference on Computer Vision and Pattern Recognition, CVPR 2018, Salt Lake City, UT, USA, June 18-22, 2018*. Computer Vision Foundation / IEEE Computer Society, 2018, pp. 616–625.
- [105] A. Vaswani, N. Shazeer, N. Parmar, J. Uszkoreit, L. Jones, A. N. Gomez, L. Kaiser, and I. Polosukhin, “Attention is all you need,” in *Advances in Neural Information Processing Systems 30: Annual Conference on Neural Information Processing Systems 2017, December 4-9, 2017, Long Beach, CA, USA, 2017*, pp. 5998–6008.
- [106] A. Kirillov, E. Mintun, N. Ravi, H. Mao, C. Rolland, L. Gustafson, T. Xiao, S. Whitehead, A. C. Berg, W. Lo, P. Dollár, and R. B. Girshick, “Segment anything,” in *IEEE/CVF International Conference on Computer Vision, ICCV 2023, Paris, France, October 1-6, 2023*. IEEE, 2023, pp. 3992–4003.
- [107] A. Radford, J. W. Kim, C. Hallacy, A. Ramesh, G. Goh, S. Agarwal, G. Sastry, A. Askell, P. Mishkin, J. Clark, G. Krueger, and I. Sutskever, “Learning transferable visual models from natural language supervision,” in *Proceedings of the 38th International Conference on Machine Learning, ICML 2021, 18-24 July 2021, Virtual Event*, ser. Proceedings of Machine Learning Research, vol. 139. PMLR, 2021, pp. 8748–8763.
- [108] S. Ren, K. He, R. B. Girshick, and J. Sun, “Faster R-CNN: towards real-time object detection with region proposal networks,” in *Advances in Neural Information Processing Systems 28: Annual Conference on Neural Information Processing Systems 2015, December 7-12, 2015, Montreal, Quebec, Canada, 2015*, pp. 91–99.
- [109] T. Lin, M. Maire, S. J. Belongie, J. Hays, P. Perona, D. Ramanan, P. Dollár, and C. L. Zitnick, “Microsoft COCO: common objects in context,” in *Computer Vision - ECCV 2014 - 13th European Conference, Zurich, Switzerland, September 6-12, 2014, Proceedings, Part V*, ser. Lecture Notes in Computer Science, vol. 8693. Springer, 2014, pp. 740–755.
- [110] M. Caron, H. Touvron, I. Misra, H. Jégou, J. Mairal, P. Bojanowski, and A. Joulin, “Emerging properties in self-supervised vision transformers,” in *2021 IEEE/CVF International Conference on Computer Vision, ICCV 2021, Montreal, QC, Canada, October 10-17, 2021*. IEEE, 2021, pp. 9630–9640.
- [111] A. Dosovitskiy, L. Beyer, A. Kolesnikov, D. Weissenborn, X. Zhai, T. Unterthiner, M. Dehghani, M. Minderer, G. Heigold, S. Gelly, J. Uszkoreit, and N. Houlsby, “An image is worth 16x16 words: Transformers for image recognition at scale,” in *9th International Conference on Learning Representations, ICLR 2021, Virtual Event, Austria, May 3-7, 2021*. OpenReview.net, 2021.
- [112] K. He, X. Chen, S. Xie, Y. Li, P. Dollár, and R. B. Girshick, “Masked autoencoders are scalable vision learners,” in *IEEE/CVF Conference on Computer Vision and Pattern Recognition, CVPR 2022, New Orleans, LA, USA, June 18-24, 2022*. IEEE, 2022, pp. 15 979–15 988.
- [113] C. Schuhmann, R. Beaumont, R. Vencu, C. Gordon, R. Wightman, M. Cherti, T. Coombes, A. Katta, C. Mullis, M. Wortsman, P. Schramowski, S. Kundurthy, K. Crowson, L. Schmidt, R. Kaczmarczyk, and J. Jitsev, “LAION-5B: an open large-scale dataset for training next generation image-text models,” in *NeurIPS*, 2022.
- [114] A. van den Oord, Y. Li, and O. Vinyals, “Representation learning with contrastive predictive coding,” *CoRR*, vol. abs/1807.03748, 2018.
- [115] S. Liu, Z. Zeng, T. Ren, F. Li, H. Zhang, J. Yang, Q. Jiang, C. Li, J. Yang, H. Su, J. Zhu, and L. Zhang, “Grounding DINO: marrying DINO with grounded pre-training for open-set object detection,” in *Computer Vision - ECCV 2024 - 18th European Conference, Milan, Italy, September 29-October 4, 2024, Proceedings, Part XLVII*, ser. Lecture Notes in Computer Science, vol. 15105. Springer, 2024, pp. 38–55.
- [116] Y. Li, H. Wang, Y. Duan, and X. Li, “CLIP surgery for better explainability with enhancement in open-vocabulary tasks,” *CoRR*, vol. abs/2304.05653, 2023.
- [117] C. Zhou, C. C. Loy, and B. Dai, “Extract free dense labels from CLIP,” in *Computer Vision - ECCV 2022 - 17th European Conference, Tel Aviv, Israel, October 23-27, 2022, Proceedings, Part XXVIII*, ser. Lecture Notes in Computer Science, vol. 13688. Springer, 2022, pp. 696–712.
- [118] H. Idrees, M. Tayyab, K. Athrey, D. Zhang, S. Al-Máadeed, N. M. Rajpoot, and M. Shah, “Composition loss for counting, density map estimation and localization in dense crowds,” in *Computer Vision - ECCV 2018 - 15th European Conference, Munich, Germany, September 8-14, 2018, Proceedings, Part II*, ser. Lecture Notes in Computer Science, vol. 11206. Springer, 2018, pp. 544–559.
- [119] R. Guerrero-Gómez-Olmedo, B. Torre-Jiménez, R. J. López-Sastre, S. Maldonado-Bascón, and D. Oñoro-Rubio, “Extremely overlapping vehicle counting,” in *Pattern Recognition and Image Analysis - 7th Iberian Conference, IbPRIA 2015, Santiago de Compostela, Spain, June 17-19, 2015, Proceedings*, ser. Lecture Notes in Computer Science, vol. 9117. Springer, 2015, pp. 423–431.
- [120] L. Ciampi, C. Santiago, J. Costeira, C. Genaro, and G. Amato, “Night and Day Instance Segmented Park (NDISPark) Dataset: a Collection of

- Images taken by Day and by Night for Vehicle Detection, Segmentation and Counting in Parking Areas,” May 2022.
- [121] L. Ciampi, V. Zeni, L. Incrocci, A. Canale, G. Benelli, F. Falchi, G. Amato, and S. Chessa, “Pest sticky traps: a dataset for whitefly pest population density estimation in chromotropic sticky traps,” Apr. 2023.
- [122] A. Mondal, S. Nag, X. Zhu, and A. Dutta, “Omnicon: Multi-label object counting with semantic-geometric priors,” in *AAAI-25, Sponsored by the Association for the Advancement of Artificial Intelligence, February 25 - March 4, 2025, Philadelphia, PA, USA*. AAAI Press, 2025, pp. 19 537–19 545.
- [123] M. A. Hobley and V. Prisacariu, “ABC easy as 123: A blind counter for exemplar-free multi-class class-agnostic counting,” in *Computer Vision - ECCV 2024 - 18th European Conference, Milan, Italy, September 29-October 4, 2024, Proceedings, Part XI*, ser. Lecture Notes in Computer Science, vol. 15069. Springer, 2024, pp. 304–319.
- [124] A. C. D’Alessandro, A. Mahdavi-Amiri, and G. Hamarneh, “Afreca: Annotation-free counting for all,” in *Computer Vision - ECCV 2024 - 18th European Conference, Milan, Italy, September 29-October 4, 2024, Proceedings, Part IV*, ser. Lecture Notes in Computer Science, vol. 15062. Springer, 2024, pp. 75–91.
- [125] P. Doubinsky, N. Audebert, M. Crucianu, and H. L. Borgne, “Semantic generative augmentations for few-shot counting,” in *IEEE/CVF Winter Conference on Applications of Computer Vision, WACV 2024, Waikoloa, HI, USA, January 3-8, 2024*. IEEE, 2024, pp. 5431–5440.
- [126] L. Ciampi, N. Messina, M. Pierucci, G. Amato, M. Avvenuti, and F. Falchi, “Mind the prompt: A novel benchmark for prompt-based class-agnostic counting,” *CoRR*, vol. abs/2409.15953, 2024, accepted at IEEE Winter Conference on Applications of Computer Vision, WACV 2025.
- [127] G. Pacini, L. Bianchi, L. Ciampi, N. Messina, G. Amato, and F. Falchi, “Countingdino: A training-free pipeline for class-agnostic counting using unsupervised backbones,” *CoRR*, vol. abs/2504.16570, 2025.
- [128] L. Knobel, T. Han, and Y. M. Asano, “Learning to count without annotations,” in *IEEE/CVF Conference on Computer Vision and Pattern Recognition, CVPR 2024, Seattle, WA, USA, June 16-22, 2024*. IEEE, 2024, pp. 22 924–22 934.